From biodiversity modelling to conservation action: a spatial indicator for prioritising tropical forest protection, restoration, and management

Maïri Souza Oliveira[a,b]*, Maxime Lenormand[a*], Sandra Luque[a]

[a]INRAE, National Research Institute on Agriculture, Food & the Environment, TETIS research unit, Maison de la télédétection, 34090 Montpellier, France

[b]CIRAD, Centre for International Cooperation in Agricultural Research for Development, Forests and Societies research unit, Montpellier 34398, France

*Corresponding author: mairisouzaoliveira@gmail.com and maxime.lenormand@inrae.fr

Graphical abstract

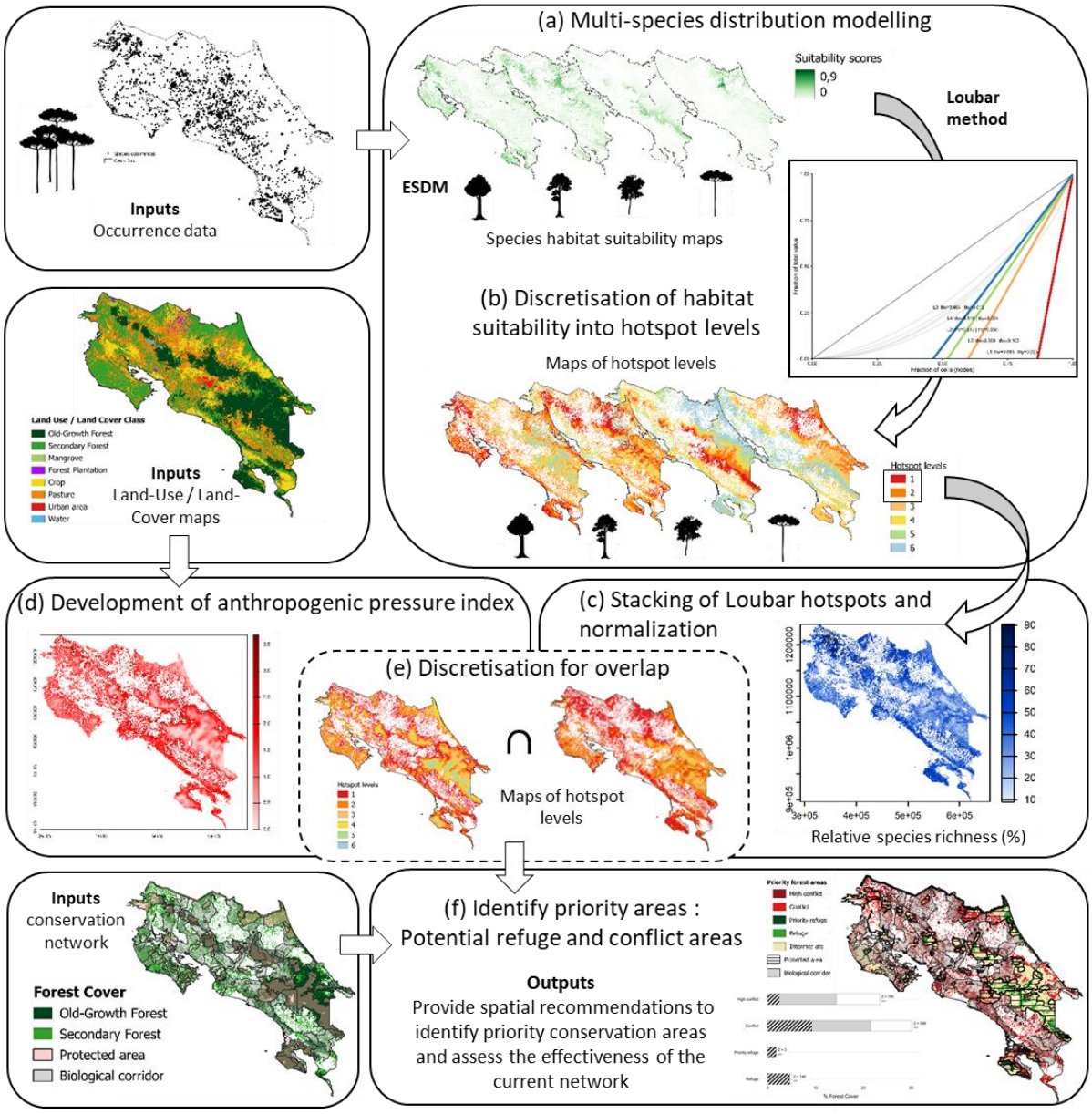

Abstract

Tropical forests harbour exceptional biodiversity but are increasingly threatened by anthropogenic pressures, making their conservation central to achieving the Convention on Biological Diversity targets. However, national conservation planning is often constrained by heterogeneous monitoring frameworks and limited integration of biodiversity and anthropogenic pressures. We develop a synthetic spatial indicator that combines open-access biodiversity and land-use data to identify refuge and conflict areas between ecological potential and anthropogenic pressure. Using Costa Rica as a national-scale demonstrator, we assess its capacity to support conservation prioritisation and evaluate the current conservation network. Ecological potential was estimated using multi-species distribution models for 254 dominant canopy tree species, serving as an operational proxy for tropical forest biodiversity and ecological structure. We quantified anthropogenic pressure from land-use patterns and combined it with ecological potential to identify refuge and conflict areas. We then tested the spatial significance of these areas and evaluated their representation within the national conservation network. The indicator reveals a clear spatial organisation of biodiversity–pressure interactions: refuge areas coincide with large, continuous forest cores, whereas conflict areas are concentrated in fragmented landscapes and may extend into protected areas. Flexible and transferable, the framework distinguishes areas requiring strict protection from those where restoration, sustainable management, or pressure mitigation should be prioritised. Rather than prescribing conservation actions, the refuge–conflict indicator provides a practical decision-support tool to assess conservation networks, strengthen ecological connectivity, and guide national biodiversity planning.

Key words

Ecological indicator; Conservation prioritisation; Species distribution modelling; Anthropogenic pressure; Kunming-Montreal Global Biodiversity Framework; Forest integrity; Refuge-conflict framework

1. Introduction

Tropical forests harbor a major share of terrestrial biodiversity, while being subject to increasing pressures that are driving an alarming erosion of this biodiversity (Barlow et al., 2018; Gibson et al., 2011). Biodiversity loss is primarily due to human activities leading to land conversion, landscape fragmentation and degradation, and climate change (Caro et al., 2022; Curtis et al., 2018; FAO, 2025; Pendrill et al., 2022). Recent syntheses show that, beyond deforestation, the integrity and connectivity of remaining large contiguous forest areas are rapidly declining, with direct implications for species persistence and ecosystem functioning (Grantham et al., 2020). These forests are central to conservation strategies aimed at achieving the objective of the Convention on Biological Diversity (CBD – COP15), which seeks to ensure the effective protection and restoration of at least 30% of ecosystems by 2030 (CBD, 2022; Mrema et al., 2020). In this context, spatial planning must move beyond identifying priority areas and instead establish actionable priorities to guide national-scale decisions between protection (preventing loss) and restoration (recovering ecological potential) (Chazdon et al., 2024; Marshall et al., 2022; Possingham et al., 2015). The restoration ecological success depends strongly on spatial targeting, and explicit prioritisation can significantly alter the effectiveness of investments (Holl et al., 2022; Strassburg et al., 2020). However, operationalising robust prioritisation frameworks remains difficult at national scale in tropical contexts, for many reasons.

On the one hand, approaches centred on rarity or threat status (e.g. the IUCN Red List) remain constrained by taxonomic biases and data deficiencies, particularly marked for plants and many

tropical groups. Recent studies document these limitations and their consequences for extinction risk assessment and for the usability of assessments in decision-making (Borgelt et al., 2022; Thomas et al., 2024). Moreover, even when sufficient occurrence data are available, focusing solely on endemic or threatened species is insufficient. To preserve ecosystem functions, particularly structural ones, and to avoid biasing conservation strategies, it is necessary to incorporate all species, including those that are less represented or not threatened (Akçakaya et al., 2020; Rey et al., 2024; Zhang et al., 2022). Finally, frameworks such as Key Biodiversity Areas (KBA – IUCN, 2016), based on criteria encompassing the presence of threatened species, restricted-range taxa or ecosystems, intact ecosystems, essential ecological processes or demonstrated irreplaceability (Plumptre et al., 2025), although structuring, often require homogeneous datasets and implementation capacity that are not always available at national level. Moreover, the question of ecological condition of sites (forest integrity) becomes central to making these frameworks truly operational (Crowe et al., 2023).

Many prioritisation approaches for conservation rely primarily on ecological value or importance, whereas the explicit and joint integration of a spatial assessment of pressures (threats, disturbances, vulnerabilities) remains uneven and is not undertaken systematically (Grantham et al., 2020; Pla et al., 2024; Ward et al., 2020). Yet forest integrity approaches show that a significant proportion of remaining forests is already highly altered, including within protected areas. The simple presence of forest (quantitative state) does not guarantee high integrity or realistic conservation potential (qualitative state) (Edgar, 2025; Watson et al., 2018). Without coupling ecological value and anthropogenic pressure, prioritisation maps risk being of limited interpretability in terms of measures (protect vs restore vs actively manage).

Finally, a further challenge concerns the representation of biodiversity at large scale. The use of proxies is often indispensable, but their performance and limitations must be made explicit (Barlow et al., 2007). Recent analyses of Neotropical conservation prioritisation reveal spatial mismatches between priorities based on composition, structure, and function, highlighting the value of integrative proxies and the need to test their effectiveness rather than assume it (Burbano-Girón et al., 2022). In tropical forests, where exhaustive coverage of diversity is unrealistic, assemblages of dominant canopy species offer strong potential as both an operational and ecologically grounded proxy. These abundant species structure forest architecture and, at broader scales, ecosystems (Souza Oliveira et al., 2025a), modulate microclimate, and integrate broad biogeographical and edaphic gradients (Lohbeck et al., 2016; Rüger et al., 2023; ter Steege et al., 2013). Their composition synthesises functional strategies and controls major processes (carbon, water, energy, light, litter), thereby conditioning a substantial share of the environmental filters that structure the composition and realised niches of lower strata (Aguirre-Gutiérrez et al., 2025b; Balvanera et al., 2021). Changes in dominant assemblages often provide early signals of degradation or transformation, particularly in anthropised landscapes (Barlow et al., 2018). Thus, the spatial distribution of dominant species provides a coherent, continuous and updateable signal to guide prioritisation (protection vs restoration), in complement to inventories, structural indicators and field validation (Cazzolla Gatti et al., 2022; Lindenmayer et al., 2015).

Against this background, we propose an operational national prioritisation approach that translates potential multi-species distributions into a spatial indicator designed to support biodiversity conservation planning and implementation of the Kunming–Montreal Global Biodiversity Framework (GBF). In particular, the indicator is intended to inform Targets 1 (integrated spatial planning), 2 (ecosystem restoration), and 3 (effective conservation of ecologically important areas), by providing a transparent and reproducible basis for identifying areas of high conservation value and evaluating the adequacy of existing conservation networks (Unit, 2024).

The objective is to assess the extent to which a synthetic indicator, built from open-access biodiversity and land-use data together with a structuring ecological proxy, can support national conservation prioritisation and gap analyses of protected-area networks. The originality of the approach lies in the explicit integration of (i) potential ecological value derived from multi-species distribution modelling of canopy-structuring species and (ii) a gradient of anthropogenic pressure inferred from land-use patterns. By combining these complementary dimensions, the indicator distinguishes refuge areas (high ecological potential, low anthropogenic pressure), representing priorities for long-term protection, from conflict areas (high ecological potential, high anthropogenic pressure), where restoration, sustainable management, or mitigation actions are most urgently needed. Finally, we evaluate the complementarity of these priorities with the existing network of protected areas and ecological corridors to assess the effectiveness of the national conservation network and identify opportunities for improving its contribution to GBF implementation.

We implement this framework proposing workflow to be tested in Costa Rica (Figure 1a) as a national-level demonstrator to illustrate how a reproducible spatial indicator can support biodiversity reporting and conservation planning under the GBF. Designed from open-access biodiversity and land-use data, the approach is intended to be transferable to other tropical countries seeking transparent methods for identifying conservation priorities, evaluating the representativeness of protected-area networks, and supporting reporting on GBF Targets 1–3. Costa Rica provides a particularly relevant testing context because its strong climatic and altitudinal gradients generate a complex mosaic of tropical forest ecosystems, ranging from dry forests to montane wet forests (Souza Oliveira et al., 2025a). Its forest landscapes also encompass contrasting conservation situations. Old-growth forests are mainly concentrated in protected mountainous areas and secondary forests account for approximately 36% of national forest cover (Figure 1b). They are often fragmented and embedded within agricultural, pastoral, and monoculture-dominated matrices (Figure 1c - Montero et al., 2021). This configuration reflects a dynamic land-use trajectory, marked by intensive deforestation during the 1970s–1980s, subsequent forest recovery from the 1990s onward, and the implementation in 1996 of a regulatory framework prohibiting the conversion of public and private forest lands, although early successional stages remain imperfectly covered by this protection regime (Arroyo-Mora et al., 2014; Shaver et al., 2015). These ecological and socio-environmental contrasts make Costa Rica an ideal national-scale demonstrator for assessing whether the proposed indicator can consistently identify areas requiring protection (refuge areas), restoration, or improved management (conflict areas), while simultaneously evaluating the contribution of existing protected areas and ecological corridors to national conservation objectives and GBF implementation.

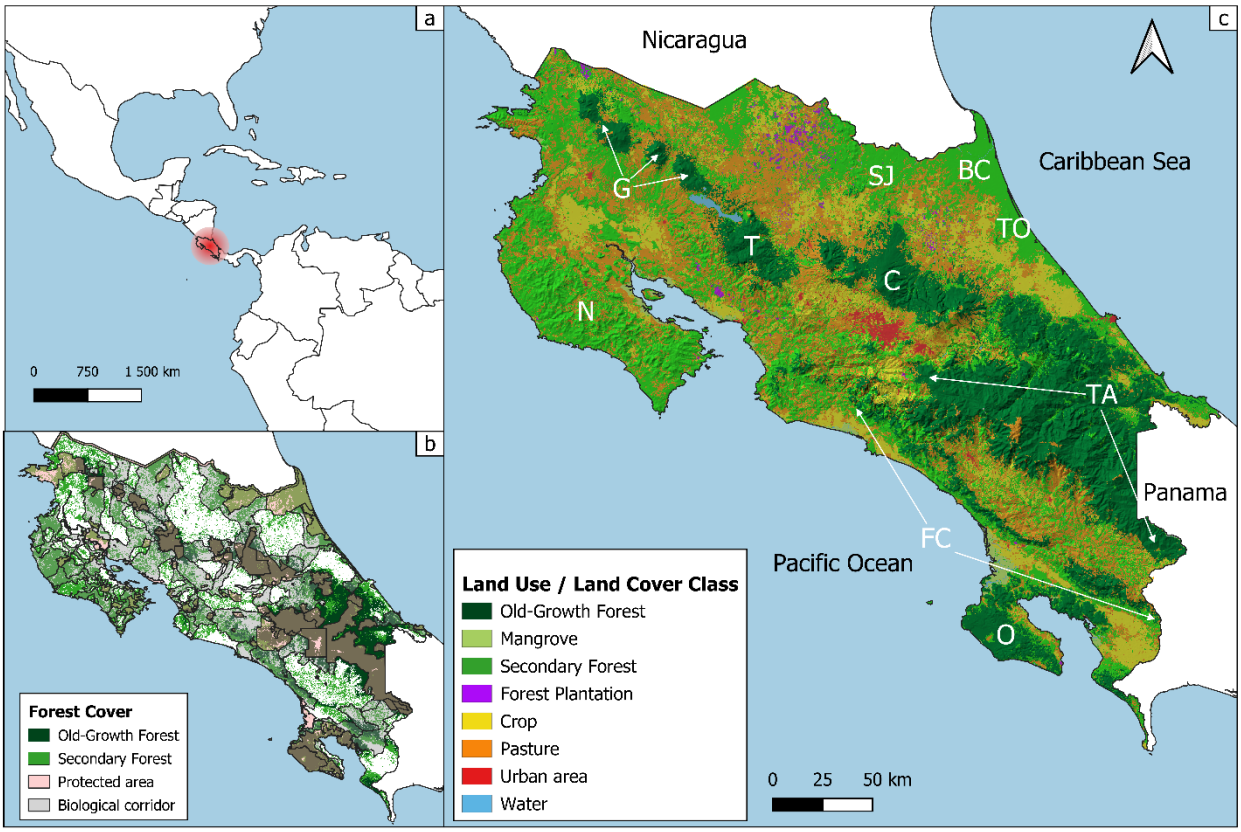

Figure 1. Spatial data context used to implement the national prioritisation framework in Costa Rica: (a) country's location in America, (b) The national forest cover in 2021 with the boundaries of protected areas, (c) reclassified SINAC land-use/land-cover map for 2017–2021 with the location of interest areas : Barra del Colorado (BC), Central mountain range (C), Fila Costeña Range (FC), Guanacaste mountain range (G), Nicoya peninsula (N), Osa peninsula (O), Biological corridor San Juan - La Selva (SJ), Tilarán mountain range (T), Talamanca mountain range (TA), Toruguero (TO).

2. Material and Methods

We therefore develop a reproducible spatial indicator designed to support national conservation planning and GBF reporting by combining open-access biodiversity and land-use land-cover data within a prioritisation framework (Figure 2). The indicator is implemented in Costa Rica as a national-scale demonstrator to assess its ability to identify refuge and conflict areas, evaluate their complementarity with protected areas and ecological corridors, and illustrate its transferability to other tropical countries.

2.1. Data

We compiled data for 367 key canopy-structuring species from the main forest ecosystems identified at the national scale in Souza Oliveira et al. (2025a) using the GBIF database (GBIF.org, 2025a-j). We extended the temporal coverage of the data from 2004 to 2025 to ensure a sufficient number of occurrences for modelling and to align with the period of the forest inventories used to delineate the main ecosystems. This approach assumes relative stability of forest cover since the 2000s, based on the Forest Law No. 7575 of 1996 (MINAE, 1996). In total, we used 18,075 occurrences, ranging from 10 to 193 per species. Details on species and occurrence numbers are provided in Figure S1 and Table S1.

To assess the potential distribution of the studied species, i.e. their abiotic ecological niche, we selected variables representing vegetation dynamics, topography, soil, and climatic conditions, as previously used in ecosystem modelling by Souza Oliveira et al. (2025a), to which the species studied contribute significantly:

- Vegetation: The Normalized Difference Water Index (NDWI) during the wet season (November to January) was calculated as the median over the 2018 multitemporal optical image series from the Copernicus Sentinel-2 L2A satellite, at 10 m and 20 m spatial resolution (CEOS, 2024), available as open access ("costarica-sentinel-2-l2-spectral-indices," n.d.).
- Topography: Elevation (m) and slope (°) were derived from the NASADEM Merged DEM Global 1 Arc-Second V001, with a spatial resolution of 30 m (NASA JPL, 2020).
- Climate: Mean annual precipitation (anPR, mm/year) and the coefficient of variation of precipitation seasonality (PRSea, %), at 1 km resolution, were obtained from CHELSA v1.0 (Karger et al., 2017).
- Soil: topsoil Cation Exchange Capacity (CEC30, mmolc/kg) and pH (pH30), at 250 m resolution, were sourced from SoilGrids v0.5.5 (Hengl et al., 2017).

To develop a spatial indicator of local anthropogenic pressure on forest cover, we calculated metrics at the class level from the Costa Rica LULC map at 10 m spatial resolution produced by SINAC (SINAC, 2021). This map was generated from a classification of Sentinel-2 and Sentinel-1 mosaics and supplemented with the 2017 LULC map for missing pixels. It was reclassified and aggregated to 250 m to ensure consistency with the resolution of habitat suitability maps (Figure 1c). The spatial layers of protected areas and biological corridors used (Figure 1b), as well as the LULC data are available freely via SNIT ("SNIT," n.d.).

2.3. Ensemble Species Distribution Models from environmental data

To identify priority areas for the studied species, we used a multi-species workflow based on species-level ensemble species distribution models (ESDM) fitted to cleaned occurrence records compiled from GBIF (Figure 2a) (GBIF.org, 2025a-j), which aggregates heterogeneous biodiversity observations including citizen-science contributions (Araújo and New, 2007; Zizka et al., 2020; Zwiener and Alves, 2023).

Environmental variables were resampled to a common spatial resolution of 250 m, with upscaled layers (NDWIw, DEM, and slope) aggregated using mean, standard deviation, and maximum values. To limit overfitting, a variable selection procedure was applied in which one variable from each group of collinear variables was selected based on Pearson correlation ($r \geq 0.7$). The same variables were selected for all species. The relative contribution of each variable, calculated independently of the modelling algorithms, corresponds to the Pearson coefficient between the initial model predictions and those obtained via a jackknife omission test of the evaluated variable (Hawkins et al., 2017).

To reduce sampling bias associated with multiple occurrences within the same pixel, presence points were spatially rarefied to match the resolution of the environmental and species data (250 m) and to avoid clustering, retaining only one randomly chosen occurrence per pixel (Souza Oliveira et al., 2025b). Following this filtering, 6,823 occurrences were retained for 254 species. The resulting species list and the number of occurrences at this spatial resolution are presented in Table S1.

For each species, 1,000 pseudo-absences were randomly generated within the background using disk stratification to avoid spatial clustering around presence points. Presences and pseudo-absences were

weighted equally in the model. This approach ensures a balanced representation of presence and absence data for the algorithms included in the ESDM.

Models were run using seven algorithms available in the SSDM R package (Schmitt et al., 2017) to improve robustness, accuracy, and stability of SDMs, accounting for uncertainty related to algorithm choice (Kaky et al., 2020; Montoya-Jiménez et al., 2022; Zurell et al., 2020). The algorithms used were: Generalised Additive Model (GAM), Generalised Linear Model (GLM), Multivariate Adaptive Regression Splines (MARS), Artificial Neural Networks (ANN), Classification Tree Analysis (CTA), Random Forest (RF), and Maximum Entropy (MAXENT). Each model was calibrated ten times and validated using holdout cross-validation, with 70 % of the data used for training and 30 % for validation, over five iterations. Habitat suitability maps for each species were produced from an ensemble model, calculated by weighting the suitability scores of individual models with an Area Under the ROC Curve (AUC) ≥ 0.7 (Hanley and McNeil, 1982).

Detecting false positives and false negatives is essential for biodiversity conservation, as overestimating or underestimating a species' potential range can lead to inappropriate management decisions (Guisan et al., 2013). We retained 119 species with a low number of occurrences (10 to 20) to include localized taxa that may be important for maximizing hotspot detection within our overall workflow (Konowalik and Nosol, 2021; Sampaio and Cavalcante, 2023; van Proosdij et al., 2016). In this context, no single metric is reliable, particularly with small samples; therefore, it is recommended to combine indicators of discrimination, calibration, bias, and accuracy (Konowalik and Nosol, 2021). To assess model quality, we selected a complementary set of three metrics suitable for adequacy scores and underrepresented species: (i) the AUC, which measures a model's ability to discriminate presence sites from absence sites; (ii) the Continuous Boyce Index (CBI), a calibration metric, which evaluates the accuracy of occurrence predictions relative to a random distribution of occurrences along the prediction gradient; and (iii) Bias, which measures the systematic deviation between predicted and observed values, calculated as the mean difference (Konowalik and Nosol, 2021; Zurell et al., 2020) (Konowalik and Nosol, 2021; Zurell et al., 2020). The ecological consistency of habitat suitability maps for species whose metrics may indicate poor model performance was evaluated through expert assessment (Zurell et al., 2020).

2.4. Development of a local anthropogenic pressure indicator derived from LULC data

To characterise local anthropogenic pressure around forest pixels, we developed a landscape-based pressure indicator derived from LULC data by combining class-level landscape metrics describing the composition and configuration of anthropogenic land-use classes (Figure 2d).

Anthropogenic pressures on forests, at both landscape and local scales, determine their ecological state and are primarily influenced by the composition and configuration of the surrounding landscape, which affect connectivity, edge effects, and biodiversity (Arroyo-Rodríguez et al., 2020; Fahrig, 2017, 2013; Rosenfield et al., 2023). Landscape metrics describing anthropogenic land-use classes thus provide robust spatial indicators to characterise these pressures and to identify conflict zones and biodiversity refuges. Fifteen class-level landscape metrics were calculated to quantify the importance and impact of each anthropogenic class (forest plantations, croplands, pastures, urban areas) on the landscape surrounding each forest pixel. The full set of metrics was selected based on their definitions in FRAGSTATS (McGarigal et al., 2022) and are presented in Table S2. We selected the focal window size for moving-window landscape metrics using a cross-scale sensitivity analysis based on three complementary indicators: (i) a spatial roughness index, (ii) global variance, and (iii) inter-scale stability quantified by correlation with the smallest window. Candidate windows, ranging from 1 km to 10 km,

were chosen with reference to spatial scales documented in the scientific literature at which anthropogenic pressures significantly affect forest patch floristic patterns, while remaining appropriate for the 250 m resolution of the data used (Grantham et al., 2020; Haddad et al., 2015). Full equations and implementation details are provided in Section S1.

Among the fifteen landscape metrics calculated, a collinearity analysis was conducted to select a set of non-collinear ($|r| < 0.8$) and complementary metrics, identified in the literature as relevant, in order to characterise the importance and influence of each class on landscape structure. The same selection was applied to all anthropogenic classes to produce comparable and subsequently combinable indices. The metrics were then standardised (z-score) and some transformed (reoriented) to ensure directional consistency across all indicators, so that increases in their values consistently corresponded to intensification of anthropogenic pressure. An independent PCA was conducted for each anthropogenic class using the standardised and directionally aligned metrics. When the first principal component explained more than 70% of the total variance, it was retained as the class-specific pressure score. Otherwise, a weighted combination of the leading components was calculated, with weights proportional to their explained variance, retaining enough components to reach 70% cumulative variance. The axes were reoriented so that increasing scores consistently reflected an intensification of anthropogenic pressure. The resulting scores were then normalised between 0 and 1 to produce a continuous index for each class, and subsequently summed to obtain the landscape-scale pressure index $P(x)$, bounded within [0,4] .

2.5. Discretisation into "hotspot" levels: construction of the Indices *b* and *p*

Continuous spatial layers generated throughout the workflow, namely habitat suitability scores, relative species richness, and anthropogenic pressure, were represented as raster maps. Because these variables differed in scale, range, and distribution, and often showed highly skewed spatial patterns, direct comparison or overlay was not straightforward. To preserve the information contained in the continuous gradients while defining spatially comparable classes, we reclassified these rasters into ordered hotspot levels using the Loubar method (Louail et al., 2014), applied iteratively (Bassolas et al., 2019; Préau et al., 2022) (Figure 2b, 2e).

Let $Z(x)$ denote the value of a continuous raster at pixel x. The Loubar method relies on the analysis of the Lorenz curve of Z and on the tangent to this curve at point (1,1), allowing the non-parametric identification of thresholds that isolate the values concentrating most of the signal. By iteratively applying this procedure, each continuous raster was converted into six ordered hotspot levels:

$$H_z(x) \in \{1,2,3,4,5,6\} \quad (1)$$

where $H_z(x) = 1$ corresponds to the strongest hotspot, i.e. the highest values of Z, and $H_z(x) = 6$ corresponds to the lowest values.

2.5.1. Estimation of continuous relative species richness

For each species $s \in \{1, \dots, S\}$, the ESDM produced a continuous habitat suitability map. Rather than binarising outputs, we identified areas of high suitability for each species using Loubar reclassification applied to habitat suitability scores (Figure 2b). This provides a species-specific ordinal suitability map:

$$H_s(x) \in \{1,2,3,4,5,6\} \quad (2)$$

where $H_z(x) = 1$ corresponds to pixels with the highest suitability (niche core), levels 2–5 represent a decreasing gradient surrounding this core, level 6 groups pixels with very low suitability. This approach preserves species-specific suitability gradients while standardising their distributions into ordinal classes, enabling comparison and overlay of maps with very different spatial scales.

For each species, uncertainty associated with the probability of presence map was propagated using a Monte Carlo approach. Based on the mean and standard deviation provided by the ESDM, 1,000 random draws were generated for each pixel following a truncated normal distribution bounded between 0 and 1. These simulations allow assessment of variability in presence probabilities and quantification of confidence in the final hotspot level assignment using the Loubar method. The most frequent hotspot class across simulations was retained as the mode, and the proportion of concordant iterations provided a confidence index for each pixel.

This approach combines the central information from the ESDM with uncertainty propagation, ensuring that areas identified as hotspots best reflect the true probability of presence for each species (Araújo et al., 2019; Thuiller et al., 2019; Zurell et al., 2020). We then defined a binary high suitability indicator for each species:

$$I_s(x) = \{1,\ if\ H_s(x) \in \{1,2\}\ 0,\ else \quad (3)$$

Relative species richness was then estimated by stacking species-level high-suitability indicators:

$$B(x) = \frac{1}{S}\sum_{s=1}^{S} I_s(x) \times 100 \quad (4)$$

where $B(x)$ represents the percentage of modelled species exhibiting high suitability at pixel x. This step provides a continuous multi-species metric interpretable as relative potential species richness..

2.5.2. Combining anthropogenic pressure and potential biodiversity hotspot levels

To directly compare and overlay potential biodiversity and anthropogenic pressure on a common scale, we converted the two continuous variables $B(x)$ and $P(x)$ into ordinal hotspot levels using the Loubar method, and analysed their overlap at the pixel scale (Figure 2e).

Relative species richness and anthropogenic pressure are described respectively by continuous rasters $B(x)$ bounded within [0,100], and $P(x)$, bounded within [0,4]. Loubar discretisation was applied separately to each raster:

$$b(x) = H_B(x), b(x) \in \{1,2,3,4,5,6\} \quad (5)$$

$$p(x) = H_P(x), p(x) \in \{1,2,3,4,5,6\} \quad (6)$$

where $b(x) = 1$ indicates pixels concentrating the highest biodiversity values while$b(x) = 6$ corresponds to the lowest ; (ii) Similarly, $p(x) = 1$ to pixels experiencing the strongest anthropogenic pressure, whereas$p(x) = 6$ indicates the weakest pressure..

Each pixel x is thus characterised by an ordinal pair;

$$\big(b(x), p(x)\big) \in \{1, \dots, 6\} \times \{1, \dots, 6\} \quad (7)$$

corresponding to36 possible combinations. This cross-classification defines a discrete space describing the co-variation between potential biodiversity and anthropogenic pressure.

2.6. A posteriori calibration of “conflict/refuge” categories and assessment of spatial significance

Refuge and conflict categories (and their intensities) were not defined a priori. They were determined a posteriori from the observed structure when the combinations $\big(b(x), p(x)\big)$ were projected into the continuous space $\big(B(x), P(x)\big)$. We examined the joint distribution of the 36 combinations and their relative positioning in the (B,P) plane in order to identify coherent groupings corresponding to conflict areas (high potential biodiversity and high pressure), refuge areas (high potential biodiversity and low pressure), and intermediate situations. This calibration ensures that the ordinal classes $b(x)$ and $p(x)$ correspond to interpretable groupings in continuous space (B, P), and defines synthetic categories (refuge/conflict) adapted to the observed distributions within the study area (Figure 2f).

After calibration, the spatial significance of these zones was assessed using a shuttle-type permutation test (500 iterations), providing a Z-score for each class that measures deviation from randomness. The proportion of permutations showing an overlap equal to or greater than the observed constitutes a one-tailed p-value, indicating whether the observed spatial configuration is significantly clustered or dispersed.

All analyses were performed using R version 4.3.3 (R Core Team, 2024). Ensemble modelling was conducted with the SSDM package version 0.2.11 (Schmitt et al., 2017), and landscape metrics were calculated using the landscapemetrics package version 2.2.1 (Hesselbarth et al., 2019).

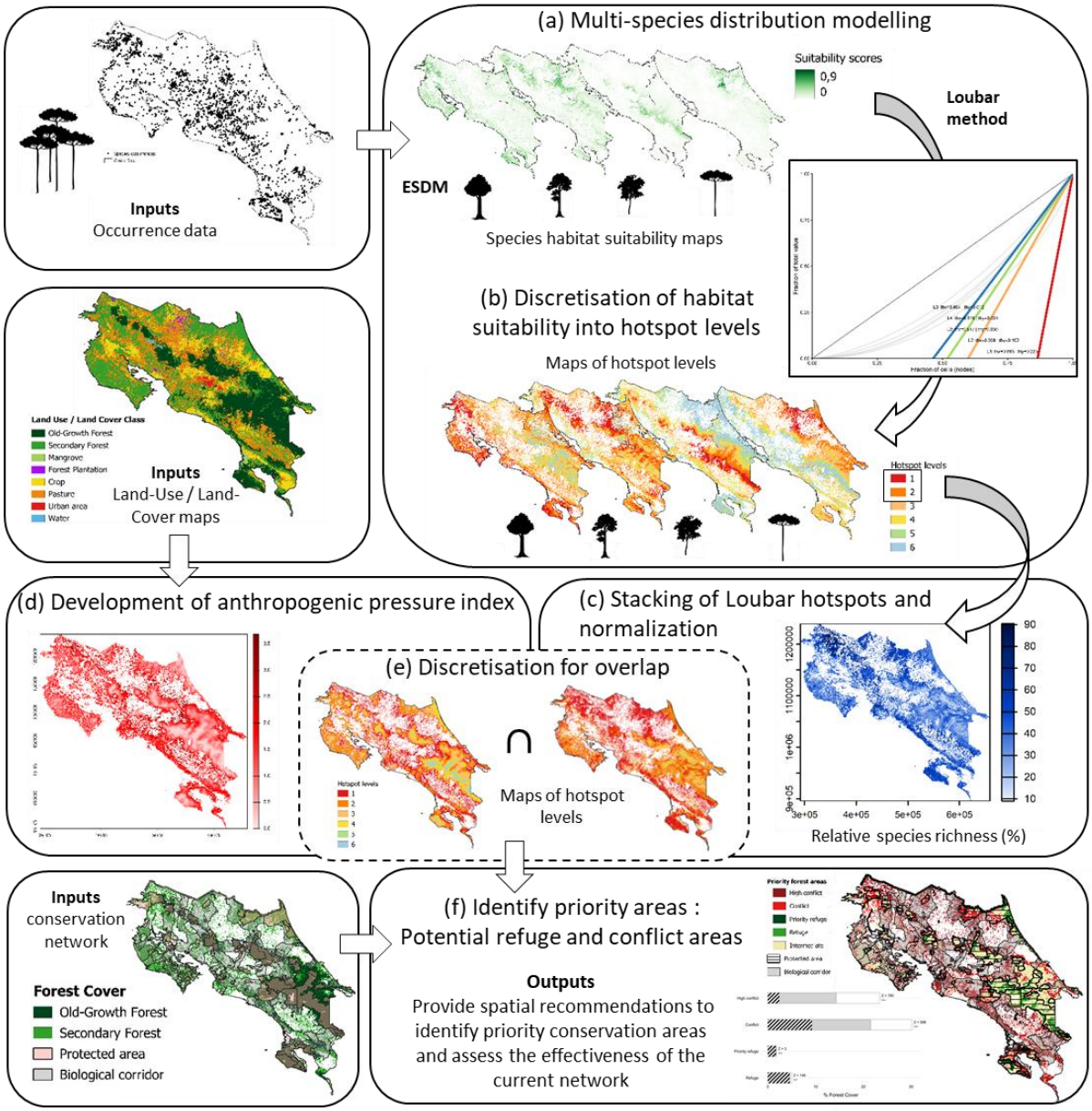

Figure 2. Schematic representation of the spatial indicator and spatial prioritisation workflow, illustrating the key methodological steps.

3. Results

3.1. Assessment of Ensemble Species Distribution Models from environmental data

All 254 species were successfully modelled, with final ESDMs selected using an AUC threshold of 0.7. Model performance was overall satisfactory, with high AUC values (0.70–0.95), low bias (< 0.18), and generally good calibration despite substantial interspecific variation in CBI (Figure S2). Five species with low calibration performance (CBI < 0.5) were further assessed through expert evaluation of habitat suitability maps to verify the ecological consistency of predictions. Figure 3 illustrates the range of ESDM outputs and the Loubar-based hotspot discretisation using four representative species with contrasting sample sizes and model performance.

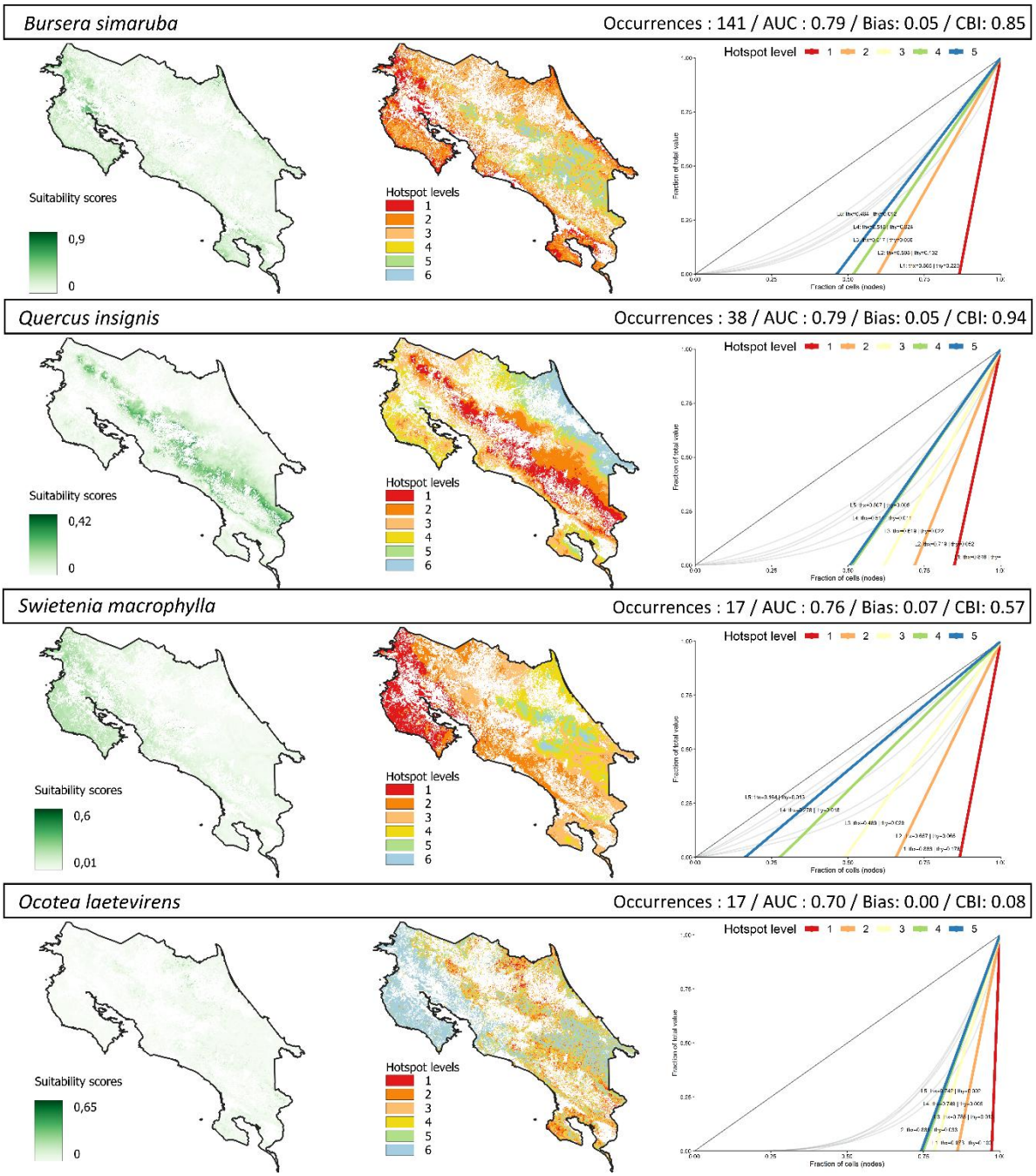

Figure 3. For four species (*Bursera simaruba, Quercus insignis, Swietenia macrophylla, Ocotea laetivirens*), this figure illustrates (i) the final habitat suitability maps produced by the ESDM (left panel), (ii) their discretisation into hotspot levels using the Loubar approach (central panel), and (iii) the corresponding Lorenz curves used to define spatial concentration thresholds (right panel). For each species, the number of occurrences used and model performance metrics (AUC, Bias, CBI) are reported in the header, spanning situations from high to very low sample sizes (down to 17 occurrences) and variable model performance.

The importance of variables varied considerably among species, with medians ranging from 7.87 % (NDWIw sd) to 14.5 % (altitude) (Figure 4). This variability was particularly pronounced for altitude, seasonal precipitation (PRSea), soil pH at 30 cm (pH30), and cation exchange capacity at 30 cm (CEC30). In contrast, some variables displayed more compact distributions (NDWIw mean, sd, anPR, and slope

mean), indicating relatively consistent importance across species. Extreme values were observed for nearly all variables, except pH30, suggesting that some species assign much greater importance to certain variables than the majority. Altitude showed the highest extreme values, with some species attributing over 50–60 % importance, while others were around 5–10 %.

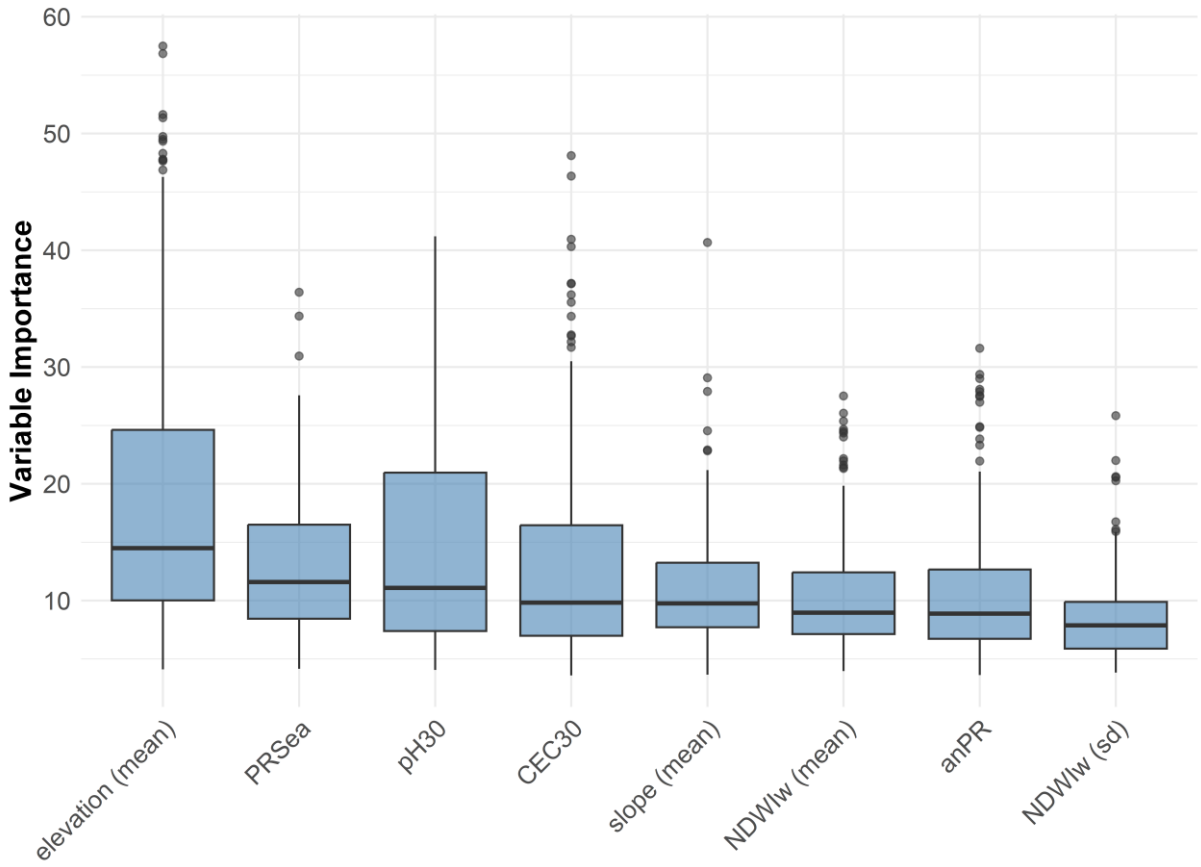

Figure 4. Distribution of the relative importance of the eight selected non-collinear environmental variables used as inputs in the SDMs.

3.2. Development of a local anthropogenic pressure indicator derived from LULC data

Cross-scale sensitivity analyses (pseudo-variogram, global variance, and inter-scale stability) converged toward a stabilisation of landscape-metric behaviour at 5 km (20 pixels), indicating limited gain in information beyond this scale and reduced noise relative to smaller windows. We therefore used a 5-km focal window for subsequent moving-window metric computations. Detailed results are provided in Figure S3. Landscape metrics at the class level were therefore computed using a 5 km focal window, to develop the anthropogenic pressure indices for the LULC classes Forest Plantation, Crop, Pasture, and Urban Area.

For these four anthropogenic classes, the metrics retained following the collinearity analysis ($|r| < 0.8$) were edge density (ED), number of patches (NP), the coefficient of variation of the fractal dimension index (FRAC_CV), and the minimum distance to pixels of the target class (MinDist) (Figure S4). All of them contributed significantly to the primary gradient (PC1) extracted by the class-specific PCA runs (Table 1). The first component (PC1) consistently explains over 70% of the variance, confirming the existence of a dominant gradient effectively summarising the structural variations specific to each class. The loadings associated with the metrics are all positive and of similar magnitude across classes, indicating that all descriptors change in the same direction along the pressure gradient. This

convergence reflects a highly stable internal structure: the same landscape dimensions drive variability, regardless of the anthropogenic class considered. This coherence allows PC1 to be used directly as a synthetic pressure index for each class. The resulting anthropogenic pressure indices display marked contrasts across Costa Rica (Figure 5). Croplands (Figure 5b) and pastures (Figure 5c) emerge as the main drivers of pressure within forested landscapes nationwide. Forest plantations (Figure 5a) exhibit a patchier but locally intense distribution, particularly in the north-Caribbean regions. Urban areas (Figure 5d), though spatially limited, generate high-pressure levels around the Central Valley, where the capital is located, and around major secondary cities.

Table 1. Loadings of landscape metrics—edge density (ed), number of patches (np), coefficient of variation of the fractal dimension index (frac_cv), and minimum distance to the pixel of the target class (min dist)—on the first principal component (PC1) for different anthropogenic land-use classes (forest plantation, crop, pasture, urban area). The Direction indicates the expected relationship between each metric and the anthropization gradient (+: increase with anthropization; –: decrease).

Class	ed	np	frac_cv	min dist	CP1
Forest Plantation	0.52	0.53	0.48	0.47	0.80
Crop	0.50	0.52	0.48	0.50	0.77
Pasture	0.49	0.49	0.49	0.52	0.73
Urban area	0.51	0.55	0.46	0.47	0.74
Direction	+	+	+	–	

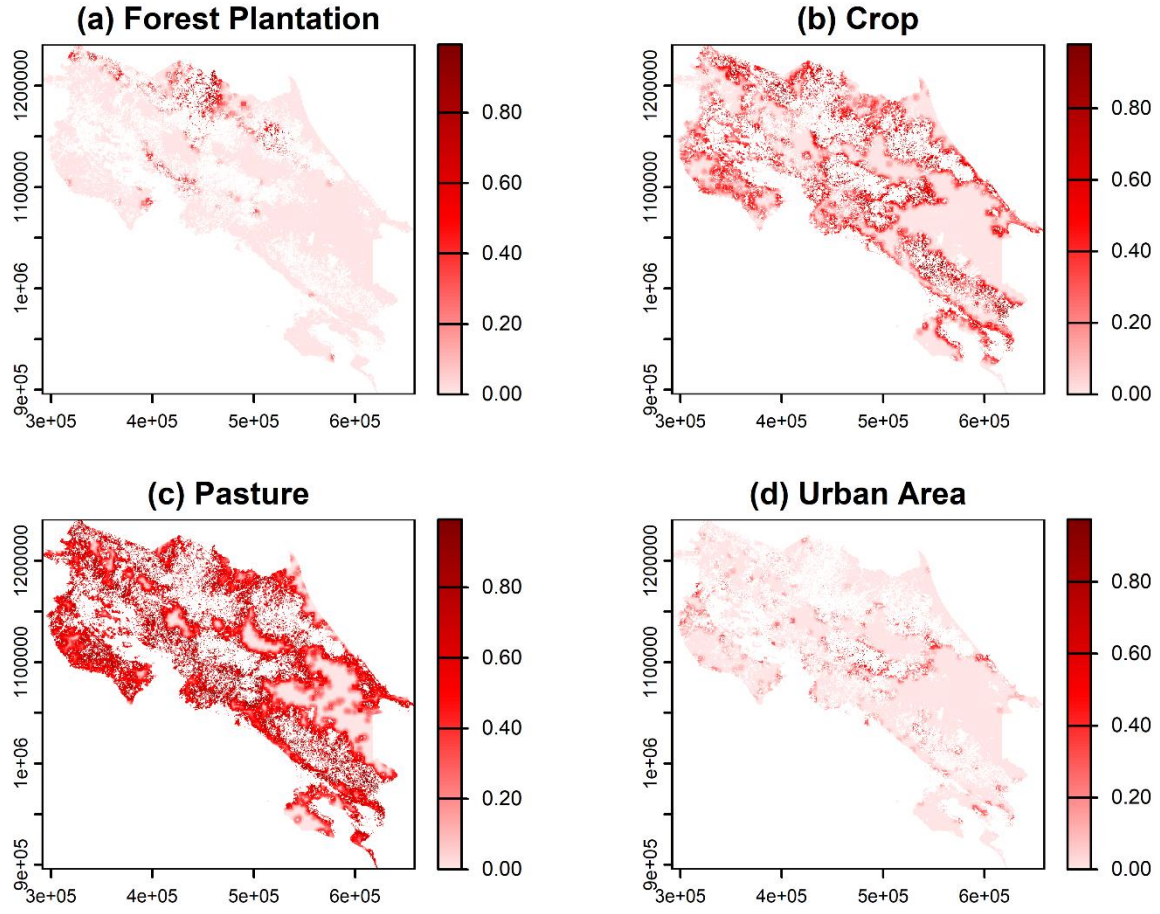

Figure 5. Anthropogenic pressure maps and distribution of forest species hotspots in Costa Rica. (a–d) Anthropogenic pressure indices derived from four LULC classes: forest plantations, croplands, pastures, and urban areas. Each index is normalized from 0 to 1 based on the same four landscape metrics: edge density (ed), number of patches (np), coefficient of variation of the fractal dimension index (frac_cv), and minimum distance to the pixel of the target class (min dist).

3.3. Mapping of conflict and refuge areas: Overlap between anthropogenic pressure and biodiversity hotspots

The overlap of hotspot levels as defined by the Loubar method for potential biodiversity b_x and actual local anthropogenic pressure p_x within Costa Rica's forest cover reveals significant spatial structuring (Figures 6 and 7).

High levels of potential biodiversity hotspots largely dominate the forest territory, with 47.6% in b_1 and 39.6% in b_2, mainly concentrated in mountainous forest complexes, the northern Caribbean coast, and the southern Pacific coast (Osa Peninsula), which may contain between 70% and 80% of species. In contrast, low levels remain marginal (< 0.5%), primarily in the Central and Talamanca mountain ranges, containing at least 8.66% of species (Figures 6a, 6c, S5). Anthropogenic pressure follows a comparable hierarchy but along a different geographical gradient. Its highest levels cover 37.7% (p_1) and 38% (p_2) of forests, especially in foothills, lowlands, and coastal areas across the country. Meanwhile, low levels (p_4 –p_6: 6.3%, 2.3%, 1.4%) are concentrated in large protected contiguous forest areas and more isolated areas (Figure 6b, c). Lorenz curves with the thresholds for each hotspot level of anthropogenic pressure and potential biodiversity are presented in Figure S6.

The associated continuous results $B(x)$ and $P(x)$, whose spatial representation is shown in Figure S5, confirm through a scatter plot a generally increasing but highly dispersed relationship between anthropogenic pressure and potential species richness. Projecting the discrete (b, p) combinations into the continuous (B, P) space highlights distinct clusters, which were used to define four operational categories a posteriori: high conflict, conflict, priority refuge, and refuge (Figure 6c; Table 2).

Table 2. Operational categories derived from combinations of biodiversity b and anthropogenic pressure p hotspot levels

Priority area	Combinations of hotspot levels	Interpretation
High conflict	b1p1	Maximum potential biodiversity and maximum anthropogenic pressure
Conflict	b1p2 , b2p1	High-to-maximum potential biodiversity and very high anthropogenic pressure
Priority refuge	b1p4 , b1p5 , b1p6	Maximum potential biodiversity and low anthropogenic pressure
Refuge	b2p4 , b2p5 , b2p6	High potential biodiversity and low anthropogenic pressure

Spatial integration of these combinations shows that high-conflict areas cover 23.42% of forest area and moderate-conflict areas 30.18%, mainly in lowlands. In contrast, priority refuges (1.76%) and refuges (4.96%) are restricted and concentrated in mountainous contiguous forest area, the Osa Peninsula, and certain northern Caribbean forests (Figure 7). Their extent departs markedly from a

random distribution ($p < 0.001$; $Z = 3–780$), revealing a strong and statistically significant spatial association between potential biodiversity hotspots and anthropogenic pressure hotspots. Finally, refuges and priority refuges remain predominantly located within protected areas (only 7.26% and 8.38% outside, including 3.36% and 1.28% within biological corridors), whereas the majority of conflict and high-conflict zones lie outside these areas (89.83% and 69.47%), including 51% and 40.8% within corridors. This pattern highlights the vulnerability of forest sectors exposed to the highest levels of anthropogenic pressure. Figure 7 reveals a recurrent spatial organisation of Costa Rica's protected continuous forests, in which protected areas are frequently surrounded by a peripheral belt of conflict zones, followed by an intermediate transition zone, and finally a core dominated by refuge and priority refuge areas. This concentric configuration suggests that the ecological integrity of protected forest cores increasingly depends on the effective management and restoration of surrounding high-pressure landscapes.

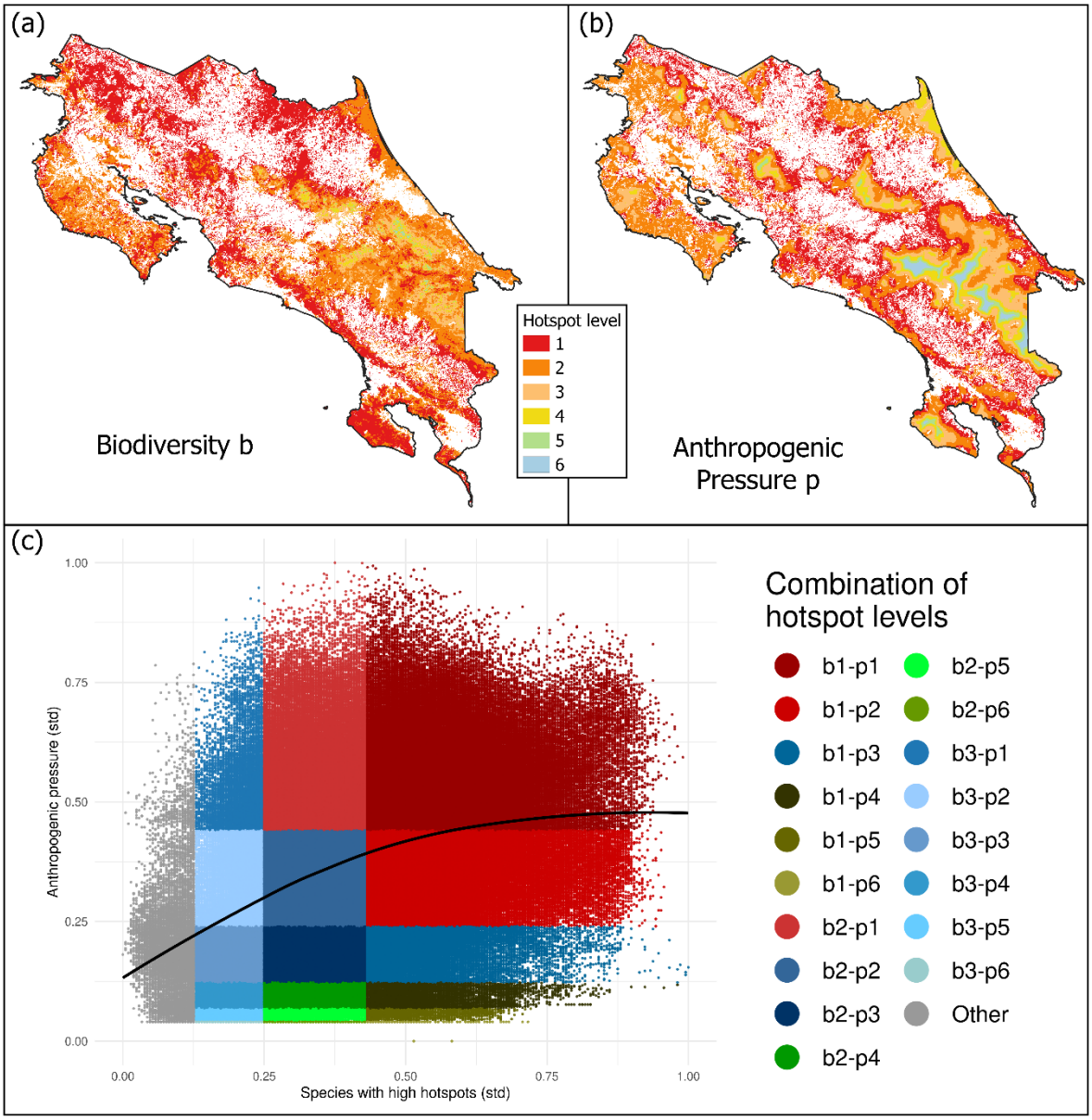

Figure 6. Overlap between potential biodiversity (b) and anthropogenic pressure (p) hotspots across the national forest cover. The hotspot maps (b) and (p), containing six loubar hotspot levels (1 = maximum intensity, 6 = minimum). The lower panel represents, for each forest pixel, the normalised intensity of anthropogenic pressure as a function of normalised species richness. Points are coloured according to their combination of hotspot levels (b–p), highlighting potential conflict

areas (red) and refuge areas (green). The loess curve illustrates the general trend between the two variables.

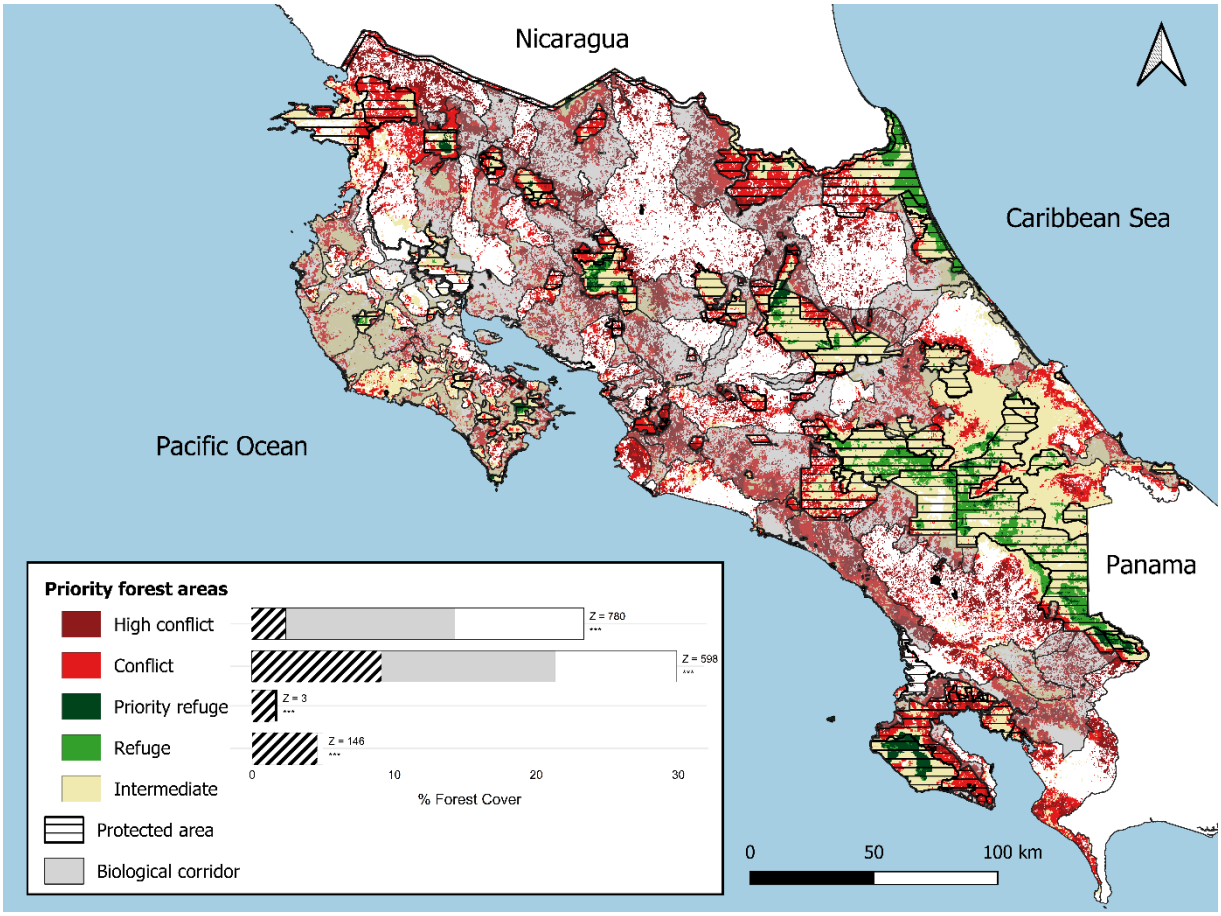

Figure 7. Map of priority forest areas in Costa Rica, identified by overlaying potential biodiversity hotspots of tree species that structure the main forest ecosystems with anthropogenic pressures at the landscape scale (5 km), with the addition of protected area boundaries. Five priority areas were distinguished: high-conflictconflict, priority biodiversity refuge, refuge, and intermediate. The adjacent bar plots show, for each category, the proportion of national forest cover, accompanied by its z-score and significance level ($p < 0.001$; ***), distinguishing surfaces within protected areas (hatched) from those outside (light grey).

4. Discussion

This study developed a reproducible, spatially explicit indicator for national biodiversity conservation planning. Designed from open-access biodiversity and land-use data, the indicator is intended to support implementation and reporting under the Kunming–Montreal Global Biodiversity Framework (GBF). It integrates potential ecological value, derived from multi-species distribution models of canopy-forming structural species used as an ecological proxy (Souza Oliveira et al., 2025a), with an index of exposure to anthropogenic pressures to identify priorities for protection, restoration, and sustainable management. Rather than aiming to provide an exhaustive representation of biodiversity, the indicator is conceived as a transparent and transferable decision-support tool that can inform spatial planning, conservation prioritisation, gap analyses of protected-area networks, and progress towards GBF Targets 1–3, which call for integrated spatial planning, ecosystem restoration, and representative, well-connected, and effectively managed conservation systems (Hughes and Grumbine, 2023; Ward et al., 2020).

4.1. Validation and interpretation of results in Costa Rica

At the scale of Costa Rica, potential refuges are concentrated within the major contiguous forest area(Figures 1, 7) already identified as priority forest cores, combining high species richness and high endemism, in national multi-taxon syntheses (Kohlmann et al., 2010) and in areas recognised as important for biodiversity (KBA) (CBD, 2021). These enclosed contiguous forest area are strongly protected and correspond to the Lowland wet evergreen forest of Caribbean slope in the Northeastern Caribbean Lowland (Barra del Colorado and Tortuguero), Wet seasonal evergreen forest on the Osa Peninsula and Premontane-to-mountain mixed-to-evergreen cloud forest in the Guanacaste, Tilarán and Central cordilleras, and Mountain oak rainforest of Talamanca (Souza Oliveira et al., 2025a). The only extensive priority refuge identified corresponds to the core of the Osa Peninsula (Corcovado National Park), confirming the importance of this region as a national hotspot of biodiversity and endemism, favoured by strong environmental and topographic variability (Gilbert and Kappelle, 2016; Hofhansl et al., 2019; Zamora et al., 2004). This strong convergence suggests that, at the national, i.e. macro-ecological, scale, despite the use of dominant canopy species as a proxy and despite biases and heterogeneity in occurrence data, the framework reproduces spatial gradients consistent with expected cores of high biodiversity value and ecological integrity (Cooper et al., 2024; Lima et al., 2026; Metcalfe et al., 2025; ter Steege et al., 2023).

Overlaying this indicator with Costa Rica's current conservation networks made it possible to identify recurrent spatial patterns within protected areas that display a high ecological value and low-pressure core (refuge), a highly exposed peripheral crown with strong ecological value (conflict), and an intermediate zone between these extremes (Figure 7). This pattern is consistent with global findings: a large proportion of protected forest areas are subject to increasing pressures and edge effects (microclimate, mortality, structural degradation), which strongly affect habitat quality, sometimes at considerable distances from the forest edge (Bourgoin et al., 2024; Grantham et al., 2020; Yang et al., 2025). In Costa Rica, a non-negligible share of conflict (10%) and high-conflict (20%) areas affects the margins of protected areas — and in some cases penetrates into them, particularly in the lowland contiguous forest area of dry deciduous forest in Guanacaste and wet evergreen forest of the Caribbean slope (San Juan–La Selva corridor), as well as part of the Osa Peninsula (Figure 1 – Souza Oliveira et al., 2025a). National assessments also acknowledge that degradation affects protected areas, due to persistent fragmentation linked in particular to the sale of usage rights ("venta de derechos") authorising agricultural, forestry or construction activities within Conservation Areas, thereby weakening the integrity of protected forests and potentially reducing their effectiveness, which may explain the observed patterns (MINAE, 2015).

The development of biological corridors is an essential strategy for maintaining connectivity among protected areas (MINAE, 2015; Morera Beita et al., 2021; Salom-Pérez et al., 2021). However, our indicator reveals that most conflict and high-conflict areas (90% and 70%, respectively) occur outside protected areas, with more than half overlapping with biological corridors. This finding highlights a potential vulnerability of the national connectivity network, as many corridor areas remain exposed to substantial anthropogenic pressures. These areas are frequently fragmented, predominantly located on private lands, and may not provide sufficiently suitable conditions to maintain the ecological functions expected from connectivity pathways for structuring species. Furthermore, existing corridors do not systematically incorporate altitudinal gradients, which are increasingly recognised as essential to facilitate species movements and climate-driven range shifts in tropical landscapes (Fung et al., 2017; Morera Beita et al., 2021). Moreover, these corridors do not always incorporate altitudinal gradients, which are essential for facilitating vertical species movements and climate-driven range shifts (Fung et al., 2017; Morera Beita et al., 2021). High-conflict areas are concentrated in fragmented forest patches embedded within agricultural lowland matrices and in some lowland–premontane forest complexes (e.g., Fila Costeña and foothill landscapes), representing multi-ecosystem areas where a high diversity of suitable niches coexist (Figures 1 and 7; Souza Oliveira et al., 2025a). Our

results therefore reveal a spatial disconnect between highly anthropised lowland landscapes, where ecological connectivity is under pressure, and residual forest refuges that are increasingly concentrated in higher-elevation forest complexes. . Low-altitude protected areas therefore appear fragmented and isolated by deforestation and agricultural expansion (McCullough et al., 2024). This configuration reflects both the legacy of agricultural colonisation and the role of topographic constraints, which have limited land-use expansion in mountainous areas, highlighting the need to strengthen connectivity and protection in low-pressure zones (Redo et al., 2012; Shaver et al., 2015). Altitude emerges as a major determinant of the distribution of many species, increasing vulnerability to warming and shifting isotherms (Aguirre-Gutiérrez et al., 2025a). In this context, cordillera refuges constitute an asset for mountain ecosystems, which are highly endemic and spatially confined. Conversely, the dry lowland forests of the north Pacific (Nicoya–Guanacaste) combine environmental constraints (altitude, PRSea) and isolation linked to agricultural expansion, increasing their sensitivity to droughts, fires and anthropogenic disturbances (Figure 1 – Souza Oliveira et al., 2025a). This issue of isolation goes beyond the case of Costa Rica: global indicators show that protected area connectivity remains a frequent shortcoming with regard to the objective of well-connected networks (Saura et al., 2018).

This interpretation provides a transferable insight for other tropical countries: the effectiveness of protected-area networks depends not only on the ecological value conserved within their boundaries, but also on the intensity of surrounding pressure gradients and the maintenance of functional connectivity across the wider landscape matrix.

4.2. Translating results into protection and restoration strategies

Within the framework of the Kunming–Montreal Global Biodiversity, which calls for integrated approaches to biodiversity protection, ecosystem restoration, and effective management by 2030 (CBD, 2022), our refuge–conflict indicator offers a reproducible decision-support tool for identifying spatially explicit conservation priorities at the national scale in tropical forest ecosystems (Figure 7).

Areas categorised as “refuges” correspond to spaces combining high potential ecological value and low anthropogenic pressure. In these sectors, the priority is to protect the ecological integrity of these core areas, followed by their spatial expansion. The literature shows that protected status does not necessarily guarantee a high level of integrity (Grantham et al., 2020; Shrestha et al., 2021). In the Costa Rican context, this implies preventing internal fragmentation, limiting authorised land-use changes within Conservation Areas, strengthening monitoring capacities, and explicitly integrating indicators of ecological value and ecological integrity into management plans (Dias et al., 2023; MINAE, 2015). Maintaining connectivity between protected areas and along altitudinal gradients also appears crucial in order to preserve species’ movement options in response to shifting isotherms (Baumbach et al., 2021; McCullough et al., 2024).

Conversely, “conflict” areas, characterised by high potential ecological value coupled with strong anthropogenic pressures, designate zones where restoration is a priority in order to promote ecological integrity and regeneration, thereby making biodiversity potential effective. In Costa Rica, these areas are mainly concentrated at the margins of protected areas, within biological corridors on private land, and in fragmented agricultural mosaics of the lowlands or premontane zones (notably Guanacaste, the Caribbean foothills and the Fila Costeña). In these contexts, the priority lies in functional restoration aimed at improving matrix permeability and reducing edge effects (Bourgoin et al., 2024; Nunes et al., 2023; Yang et al., 2025). This implies a hierarchical restoration strategy: (i) promote natural regeneration where ecologically plausible (passive restoration); (ii) deploy active restoration only where the matrix is too degraded to allow the spontaneous return of biodiversity (planting/enrichment with native and resilient species); (iii) improve matrix permeability through

agroforestry; and (iv) target incentives (PES) at corridor sections acting as bottlenecks (Chazdon et al., 2025; Cole et al., 2024; Holl et al., 2022). This interpretation is consistent with studies highlighting that biodiversity–carbon–cost restoration benefits vary greatly depending on location and cannot be optimised through simple quantitative targets (Strassburg et al., 2020).

Particular attention must be paid to interfaces between refuges and conflict areas. Where protected areas are bordered by high-pressure sectors, peripheral restoration can stabilise the intermediate zone identified in our analysis by reducing the intensity of edge effects and increasing core habitat area. This phenomenon is particularly relevant in the dry lowlands of the north Pacific, the San Juan–La Selva corridor on the northern Caribbean coast, and on the Osa Peninsula, where external fragmentation may compromise the internal ecological functionality of protected cores. The multi-species mapping produced at 250 m resolution thus makes it possible to guide, in a spatially explicit manner, action priorities across the 60% of forest cover identified as priority for the conservation of the species studied. Beyond the Costa Rican case, these results recall that the performance of a protected area network does not depend solely on the protected zone itself, but also on pressure gradients at its margins and the functional continuity of the surrounding matrix (Brennan et al., 2022; Jones et al., 2018). The refuge–conflict approach thus provides a spatially explicit workflow for moving from area-based targets to planning grounded in ecological potential, combined with integrity, connectivity and the strategic reduction of pressures.

4.3. Limitations and perspectives

Dominant canopy tree species structuring ecosystems provide a biodiversity proxy consistent with forest structure and allow identification of a significant share of potentially priority areas at national scale. However, this non-exhaustive approach may under-represent key components of biodiversity (rare, endemic, specialist, understorey species, fauna) and thus underestimate the representativeness of spatial priorities (Aguirre-Gutiérrez et al., 2025b; Barlow et al., 2007; Ritter et al., 2019; Vallé et al., 2025). Consequently, refuge–conflict maps should be viewed as a tool for identifying priority areas rather than as a complete and definitive mapping of reality. Subsequently, it will be important to test the robustness of these priority areas through an extension of the proxy to multi-taxon and/or endemic and threatened species.

This bias is amplified by the use of GBIF data, which largely rely on citizen science databases and are concentrated in accessible areas, leaving under-sampled hard-to-access regions such as the Talamanca cordillera or the northern Caribbean coastal forests, which nevertheless belong to the richest and most endemic regions. The integration of complementary data from in situ campaigns, systematic surveys or fine-scale remote sensing technologies could reduce this bias and improve the spatial accuracy of refuges (Fernández et al., 2020). However, data acquisition remains a major obstacle: high costs, lack of standardisation and coordination difficulties lead to strong disparities in in situ data, limiting countries' capacity to monitor and model biodiversity (Chapman et al., 2024).

An anthropogenic pressure index based on LULC classes and weightings effectively captures local gradients of artificialisation (deforestation, urbanisation) and may indirectly reflect certain pressures (pollution, human density) (Grantham et al., 2020). Nevertheless, it may under-represent major threats that are less visible in LULC (hunting, selective logging, fires, land-use conflicts, invasive species), and suffer from temporal mismatches between biological occurrences, infrastructure and LULC mapping. Furthermore, a purely "local" reading struggles to capture the spatio-temporal cumulative nature of direct and indirect pressures, which is nevertheless crucial for assessing vulnerability (Martini et al., 2024). It would be of interest to couple LULC-based pressure with integrity layers and more mechanistic pressure indicators; in this regard, the FLII provides a useful reference integrating observed/inferred pressures and large-scale connectivity loss (Grantham et al., 2020). This

workflow also aims to incorporate climate-change scenarios, which are essential for adaptive and forward-looking planning (Keppel et al., 2015, 2012; Selwood and Zimmer, 2020).

An often implicit limitation is that ecological prioritisation does not guarantee feasibility (opportunity costs, land tenure, governance, acceptability). Thus, the refuge–conflict indicator should be considered as a synthetic module combining potential ecological value and relative exposure to anthropogenic pressures, which can be integrated into national planning processes. It does not capture all the determining dimensions for tropical forest conservation, such as opportunity costs, land tenure and social constraints, governance capacities, or specific threats (e.g. fires, hunting and invasive species). Nevertheless, it makes explicit a central trade-off in conservation, by identifying areas where ecological potential is high but likely to be rapidly compromised by local anthropogenic pressures. Hence the relevance of this indicator in a context where expected benefits (biodiversity, carbon, costs) vary greatly depending on location and the weighting of multiple objectives (Strassburg et al., 2020). This indicator could therefore be integrated into a Systematic Conservation Planning (SCP – Plumptre et al., 2025) framework to inform multi-action zoning (protection, restoration, management, connectivity) (Baker et al., 2025; Hanson et al., 2025) with explicit connectivity indicators (Saura et al., 2018) and, where objectives are heterogeneous, support multi-criteria decision analysis approaches that make assumptions and trade-offs explicit (Cavalcante et al., 2022). In the Costa Rican case, operationalisation could be facilitated by the existence of already structured national frameworks, GRUAS and the National Biological Corridors Programme (PNCB–SINAC), which provide an institutional foundation for translating a synthetic indicator into targeting rules, scenarios and action priorities (SINAC, n.d.).

Conclusion

Ultimately, the refuge–conflict indicator should not be interpreted as a prescriptive map defining where conservation actions must occur, but rather as a transparent decision-support tool that helps reveal spatial trade-offs in tropical forest planning. By integrating ecological potential with exposure to anthropogenic pressures, it moves beyond static biodiversity mapping towards a more dynamic, risk-informed approach for prioritising conservation investments across protection, restoration, and management actions. This framework with the proposed workflow provides a reproducible and adaptable basis for supporting national biodiversity strategies, including the identification of priorities relevant to the implementation and reporting of global biodiversity targets under increasing fiscal, social, and climatic constraints.

Although its application depends on governance capacity, stakeholder engagement, and complementary socio-economic assessments, the integration of such synthetic spatial indicators into national planning processes can improve the alignment between conservation objectives and on-the-ground implementation. As tropical forests continue to face accelerating pressures and countries seek to meet ambitious biodiversity and climate commitments, approaches that make ecological priorities, underlying assumptions, and spatial trade-offs explicit will be essential for designing effective and realistic conservation strategies.

CRediT authorship contribution statement

Maïri Souza Oliveira: Conceptualization, , Data curation, Methodology, Formal analysis, Investigation, Validation, Writing – original draft, Writing – review and editing.

Maxime Lenormand: Conceptualization, Methodology, Investigation, Writing – review, Supervision.

Sandra Luque: Conceptualization, Methodology, Investigation, Writing – review and editing, Funding acquisition, Project administration, Supervision.

Acknowledgements

This research was partially funded by a PhD fellowship from INRAE (National Research Institute on Agriculture, Food & the Environment) and CIRAD (Centre for International Cooperation in Agricultural Research for Development), with additional support from CNES (National Space Agency, France) TOSCA Project CEOS-CODEX for fieldwork and data validation. We are grateful to Mona Bonier, Florian de Boissieu, Rémy Découpe, Cassio Fraga Dantas, Jean-Baptiste Féret, Renaud Marti and Simon Madec (TETIS research unit) for their valuable support in various aspects of data analysis and expertise. Thanks also to Adriana Aguilar Porras (SINAC - Sistema Nacional de Áreas de Conservación), Nelson Zamora (ITCR - Instituto Tecnológico de Costa Rica) and Diego Delgado (CATIE - Centro Agronómico Tropical de Investigación y Enseñanza) for their field expertise.

Declaration of competing interest

The authors declare that they have no known competing financial interests or personal relationships that could have appeared to influence the work reported in this paper.

Data Availability Statement

The original occurrence data were obtained from the Global Biodiversity Information Facility (GBIF) and are cited in the main text and reference list. The final dataset used in the analyses, the filtering decisions, and the processing and analysis scripts are available in the Git repository at https://github.com/ mairi-souzaoliveira /CR_refuge-conflict_areas.

References

Aguirre-Gutiérrez, J., Díaz, S., Rifai, S.W., Corral-Rivas, J.J., Nava-Miranda, M.G., González-M, R., Hurtado-M, A.B., Revilla, N.S., Vilanova, E., Almeida, E., Oliveira, E.A. de, Alvarez-Davila, E., Alves, L.F., Andrade, A.C.S. de, Costa, A.C.L. da, Vieira, S.A., Aragão, L., Arets, E., C, G.A.A., Baccaro, F., Bakker, Y.V., Baker, T.R., Bánki, O., Baraloto, C., Camargo, P.B. de, Berenguer, E., Blanc, L., Bonal, D., Bongers, F., Bordin, K.M., Brienen, R., Brown, F., Prestes, N.C.C.S., Castilho, C.V., Ribeiro, S.C., Souza, Fernanda Coelho de, Comiskey, J.A., Valverde, F.C., Müller, S.C., Silva, R. da C., Vale, J.D. do, Kamimura, V. de A., Perdiz, R. de O., Pasquel, J. del A., Derroire, G., Fiore, A.D., Disney, M., Farfan-Rios, W., Fauset, S., Feldpausch, T.R., Ramos, R.F., Llampazo, G.F., Martins, V.F., Fortunel, C., Cabrera, K.G., Barroso, J.G., Hérault, B., Herrera, R., Coronado, E.N.H., Huamantupa-Chuquimaco, I., Pipoly, J.J., Zanini, K.J., Jiménez, E., Joly, C.A., Kalamandeen, M., Klipel, J., Levesley, A., Oviedo, W.L., Magnusson, W.E., Santos, R.M. dos, Marimon, B.S., Marimon-Junior, B.H., Reis, S.M. de A., Cruz, O.A.M., Mendoza, A.M., Morandi, P., Muscarella, R., Nascimento, H., Neill, D.A., Menor, I.O., Palacios, W.A., Palacios-Ramos, S., Camacho, N.C.P., Pardo, G., Pennington, R.T., Pereira, L. de O., Pickavance, G., Picolotto, R.C., Pitman, N.C.A., Prieto, A., Quesada, C., Ramírez-Angulo, H., Réjou-Méchain, M., Correa, Z.R., Huaymacari, J.M.R., Rodriguez, C.R., Rivas-Torres, G., Roopsind, A., Rudas, A., Negret, B.S., Sande, M.T. van der, Santana, F.D., Santos, F.A.M., Bergamin, R.S., Silman, M.R., Silva, C., Espejo, J.S., Silveira, M., Souza, Fernanda Cristina, Sullivan, M.J.P., Swamy, V., Talbot, J., Terborgh, J.J., Meer, P.J. van der, Heijden, G. van der, Ulft, B. van, Martinez, R.V., Vedovato, L., Vleminckx, J., Vos, V.A., Wortel, V., Zuidema, P.A., Zwerts, J.A., Laurance, S.G.W., Laurance, W.F., Chave, J., Dalling, J.W., Barlow, J., Poorter, L., Enquist, B.J., Steege, H. ter, Phillips, O.L., Galbraith, D., Malhi, Y., 2025a. Tropical forests in the Americas are changing too slowly to track climate change. Science. https://doi.org/10.1126/science.adl5414

Aguirre-Gutiérrez, J., Rifai, S.W., Deng, X., ter Steege, H., Thomson, E., Corral-Rivas, J.J., Guimaraes, A.F., Muller, S., Klipel, J., Fauset, S., Resende, A.F., Wallin, G., Joly, C.A., Abernethy, K., Adu-Bredu, S., Alexandre Silva, C., de Oliveira, E.A., Almeida, D.R.A., Alvarez-Davila, E., Asner, G.P., Baker, T.R.,

Benchimol, M., Bentley, L.P., Berenguer, E., Blanc, L., Bonal, D., Bordin, K., Borges de Lima, R., Both, S., Cabezas Duarte, J., Cardoso, D., de Lima, H.C., Cavalheiro, L., Cernusak, L.A., dos Santos Prestes, N.C.C., da Silva Zanzini, A.C., da Silva, R.J., dos Santos Alves da Silva, R., de Andrade Iguatemy, M., De Sousa Oliveira, T.C., Dechant, B., Derroire, G., Dexter, K.G., Rodrigues, D.J., Espírito-Santo, M., Silva, L.F., Domingues, T.F., Ferreira, J., Simon, M.F., Girardin, C.A.J., Hérault, B., Jeffery, K.J., Kalpuzha Ashtamoorthy, S., Kavidapadinjattathil Sivadasan, A., Klitgaard, B., Laurance, W.F., Dan, M.L., Magnusson, W.E., Campos-Filho, E.M., Manoel dos Santos, R., Manzatto, A.G., Silveira, M., Marimon-Junior, B.H., Martin, R.E., Vieira, D.L.M., Metzker, T., Milliken, W., Moonlight, P., Moraes de Seixas, M.M., Morandi, P.S., Muscarella, R., Nava-Miranda, M.G., Nyirambangutse, B., Silva, J.O., Oliveras Menor, I., Francisco Pena Rodrigues, P.J., Pereira de Oliveira, C., Pereira Zanzini, L., Peres, C.A., Punjayil, V., Quesada, C.A., Réjou-Méchain, M., Riutta, T., Rivas-Torres, G., Rosa, C., Salinas, N., Bergamin, R.S., Marimon, B.S., Shenkin, A., Silva Rodrigues, P.M., Figueiredo, A.E.S., Garcia, Q.S., Spósito, T., Storck-Tonon, D., Sullivan, M.J.P., Svátek, M., Vieira Santiago, W.T., Arn Teh, Y., Theruvil Parambil Sivan, P., Nascimento, M.T., Veenendaal, E., Zo-Bi, I.C., Dago, M.R., Traoré, S., Patacca, M., Badouard, V., de Padua Chaves e Carvalho, S., White, L.J.T., Zhang-Zheng, H., Zibera, E., Zwerts, J.A., Burslem, D.F.R.P., Silman, M., Chave, J., Enquist, B.J., Barlow, J., Phillips, O.L., Coomes, D.A., Malhi, Y., 2025b. Canopy functional trait variation across Earth's tropical forests. Nature 641, 129–136. https://doi.org/10.1038/s41586-025-08663-2

Akçakaya, H.R., Rodrigues, A.S.L., Keith, D.A., Milner-Gulland, E.J., Sanderson, E.W., Hedges, S., Mallon, D.P., Grace, M.K., Long, B., Meijaard, E., Stephenson, P.J., 2020. Assessing ecological function in the context of species recovery. Conservation Biology 34, 561–571. https://doi.org/10.1111/cobi.13425

Araújo, M.B., Anderson, R.P., Márcia Barbosa, A., Beale, C.M., Dormann, C.F., Early, R., Garcia, R.A., Guisan, A., Maiorano, L., Naimi, B., O'Hara, R.B., Zimmermann, N.E., Rahbek, C., 2019. Standards for distribution models in biodiversity assessments. Science Advances 5, eaat4858. https://doi.org/10.1126/sciadv.aat4858

Araújo, M.B., New, M., 2007. Ensemble forecasting of species distributions. Trends Ecol Evol 22, 42–47. https://doi.org/10.1016/j.tree.2006.09.010

Arroyo-Mora, J., Svob, S., Kalacska, M., Chazdon, R., 2014. Historical Patterns of Natural Forest Management in Costa Rica: The Good, the Bad and the Ugly. Forests 5, 1777–1797. https://doi.org/10.3390/f5071777

Arroyo-Rodríguez, V., Fahrig, L., Tabarelli, M., Watling, J.I., Tischendorf, L., Benchimol, M., Cazetta, E., Faria, D., Leal, I.R., Melo, F.P.L., Morante-Filho, J.C., Santos, B.A., Arasa-Gisbert, R., Arce-Peña, N., Cervantes-López, M.J., Cudney-Valenzuela, S., Galán-Acedo, C., San-José, M., Vieira, I.C.G., Slik, J.W.F., Nowakowski, A.J., Tscharntke, T., 2020. Designing optimal human-modified landscapes for forest biodiversity conservation. Ecology Letters 23, 1404–1420. https://doi.org/10.1111/ele.13535

Baker, D.J., Gaston, K.J., Metcalfe, K., Maclean, I.M.D., 2025. Systematic conservation planning for nature recovery. BioScience 75, 472–489. https://doi.org/10.1093/biosci/biaf030

Balvanera, P., Paz, H., Arreola-Villa, F., Bhaskar, R., Bongers, F., Cortés, S., del Val, E., García-Frapolli, E., Gavito, M.E., González-Esquivel, C.E., Martínez-Ramos, M., Martínez-Yrizar, A., Mora, F., Naime, J., Pascual-Ramírez, F., Pérez-Cárdenas, N., Ugartechea-Salmerón, O.A., Siddique, I., Suazo-Ortuño, I., Swinton, S.M., 2021. Social ecological dynamics of tropical secondary forests. Forest Ecology and Management 496, 119369. https://doi.org/10.1016/j.foreco.2021.119369

Barlow, J., França, F., Gardner, T.A., Hicks, C.C., Lennox, G.D., Berenguer, E., Castello, L., Economo, E.P., Ferreira, J., Guénard, B., Gontijo Leal, C., Isaac, V., Lees, A.C., Parr, C.L., Wilson, S.K., Young, P.J.,

Graham, N.A.J., 2018. The future of hyperdiverse tropical ecosystems. Nature 559, 517–526. https://doi.org/10.1038/s41586-018-0301-1

Barlow, J., Gardner, T.A., Araujo, I.S., Ávila-Pires, T.C., Bonaldo, A.B., Costa, J.E., Esposito, M.C., Ferreira, L.V., Hawes, J., Hernandez, M.I.M., Hoogmoed, M.S., Leite, R.N., Lo-Man-Hung, N.F., Malcolm, J.R., Martins, M.B., Mestre, L.A.M., Santos, R.M.-, Nunes-Gutjahr, A.L., Overal, W.L., Parry, L., Peters, S.L., Ribeiro-Junior, M.A., Silva, M.N.F. da, Motta, C. da S., Peres, C.A., 2007. Quantifying the Biodiversity Value of Tropical Primary, Secondary, and Plantation Forests. Proceedings of the National Academy of Sciences of the United States of America 104, 18555–18560.

Bassolas, A., Barbosa-Filho, H., Dickinson, B., Dotiwalla, X., Eastham, P., Gallotti, R., Ghoshal, G., Gipson, B., Hazarie, S.A., Kautz, H., Kucuktunc, O., Lieber, A., Sadilek, A., Ramasco, J.J., 2019. Hierarchical organization of urban mobility and its connection with city livability. Nat Commun 10, 4817. https://doi.org/10.1038/s41467-019-12809-y

Baumbach, L., Warren, D.L., Yousefpour, R., Hanewinkel, M., 2021. Climate change may induce connectivity loss and mountaintop extinction in Central American forests. Commun Biol 4, 869. https://doi.org/10.1038/s42003-021-02359-9

Borgelt, J., Dorber, M., Høiberg, M.A., Verones, F., 2022. More than half of data deficient species predicted to be threatened by extinction. Commun Biol 5, 679. https://doi.org/10.1038/s42003-022-03638-9

Bourgoin, C., Ceccherini, G., Girardello, M., Vancutsem, C., Avitabile, V., Beck, P.S.A., Beuchle, R., Blanc, L., Duveiller, G., Migliavacca, M., Vieilledent, G., Cescatti, A., Achard, F., 2024. Human degradation of tropical moist forests is greater than previously estimated. Nature 631, 570–576. https://doi.org/10.1038/s41586-024-07629-0

Brennan, A., Naidoo, R., Greenstreet, L., Mehrabi, Z., Ramankutty, N., Kremen, C., 2022. Functional connectivity of the world's protected areas. Science 376, 1101–1104. https://doi.org/10.1126/science.abl8974

Burbano-Girón, J., Jantke, K., Molina-Berbeo, M.A., Buriticá-Mejía, N., Urbina-Cardona, J.N., Sánchez-Clavijo, L.M., Etter, A., 2022. An assessment of spatial conservation priorities for biodiversity attributes: Composition, structure, and function of Neotropical biodiversity. Biological Conservation 265, 109421. https://doi.org/10.1016/j.biocon.2021.109421

Caro, T., Rowe, Z., Berger, J., Wholey, P., Dobson, A., 2022. An inconvenient misconception: Climate change is not the principal driver of biodiversity loss. Conservation Letters 15, e12868. https://doi.org/10.1111/conl.12868

Cavalcante, R.B.L., Nunes, S., Viademonte, S., Rodrigues, C.M.F., Gomes, W.C., Ferreira, J. da S., Pontes, P.R.M., Giannini, T.C., Awade, M., de S. Miranda, L., Nascimento, W.R., 2022. Multicriteria approach to prioritize forest restoration areas for biodiversity conservation in the eastern Amazon. Journal of Environmental Management 318, 115590. https://doi.org/10.1016/j.jenvman.2022.115590

Cazzolla Gatti, R., Reich, P.B., Gamarra, J.G.P., Crowther, T., Hui, C., Morera, A., Bastin, J.-F., de-Miguel, S., Nabuurs, G.-J., Svenning, J.-C., Serra-Diaz, J.M., Merow, C., Enquist, B., Kamenetsky, M., Lee, J., Zhu, J., Fang, J., Jacobs, D.F., Pijanowski, B., Banerjee, A., Giaquinto, R.A., Alberti, G., Almeyda Zambrano, A.M., Alvarez-Davila, E., Araujo-Murakami, A., Avitabile, V., Aymard, G.A., Balazy, R., Baraloto, C., Barroso, J.G., Bastian, M.L., Birnbaum, P., Bitariho, R., Bogaert, J., Bongers, F., Bouriaud, O., Brancalion, P.H.S., Brearley, F.Q., Broadbent, E.N., Bussotti, F., Castro da Silva, W., César, R.G., Češljar, G., Chama Moscoso, V., Chen, H.Y.H., Cienciala, E., Clark, C.J., Coomes, D.A., Dayanandan, S., Decuyper, M., Dee, L.E., Del Aguila Pasquel, J., Derroire, G., Djuikouo, M.N.K., Van Do, T., Dolezal, J., Đorđević, I.Đ., Engel,

J., Fayle, T.M., Feldpausch, T.R., Fridman, J.K., Harris, D.J., Hemp, A., Hengeveld, G., Herault, B., Herold, M., Ibanez, T., Jagodzinski, A.M., Jaroszewicz, B., Jeffery, K.J., Johannsen, V.K., Jucker, T., Kangur, A., Karminov, V.N., Kartawinata, K., Kennard, D.K., Kepfer-Rojas, S., Keppel, G., Khan, M.L., Khare, P.K., Kileen, T.J., Kim, H.S., Korjus, H., Kumar, Amit, Kumar, Ashwani, Laarmann, D., Labrière, N., Lang, M., Lewis, S.L., Lukina, N., Maitner, B.S., Malhi, Y., Marshall, A.R., Martynenko, O.V., Monteagudo Mendoza, A.L., Ontikov, P.V., Ortiz-Malavasi, E., Pallqui Camacho, N.C., Paquette, A., Park, M., Parthasarathy, N., Peri, P.L., Petronelli, P., Pfautsch, S., Phillips, O.L., Picard, N., Piotto, D., Poorter, L., Poulsen, J.R., Pretzsch, H., Ramírez-Angulo, H., Restrepo Correa, Z., Rodeghiero, M., Rojas Gonzáles, R.D.P., Rolim, S.G., Rovero, F., Rutishauser, E., Saikia, P., Salas-Eljatib, C., Schepaschenko, D., Scherer-Lorenzen, M., Šebeň, V., Silveira, M., Slik, F., Sonké, B., Souza, A.F., Stereńczak, K.J., Svoboda, M., Taedoumg, H., Tchebakova, N., Terborgh, J., Tikhonova, E., Torres-Lezama, A., van der Plas, F., Vásquez, R., Viana, H., Vibrans, A.C., Vilanova, E., Vos, V.A., Wang, H.-F., Westerlund, B., White, L.J.T., Wiser, S.K., Zawiła-Niedźwiecki, T., Zemagho, L., Zhu, Z.-X., Zo-Bi, I.C., Liang, J., 2022. The number of tree species on Earth. Proceedings of the National Academy of Sciences 119, e2115329119. https://doi.org/10.1073/pnas.2115329119

CBD, 2022. Kunming-Montreal Global Biodiversity Framework.

CBD, 2021. Aichi Biodiversity Target 11 Country Dossier: COSTA RICA.

CEOS, 2024. Tropical Forests: Costa Rican Ecosystem Extent Demonstrator | CEOS | Committee on Earth Observation Satellites [WWW Document]. URL https://ceos.org/news/tropical-forests-costa-rica/ (accessed 12.15.24).

Chapman, M., Goldstein, B.R., Schell, C.J., Brashares, J.S., Carter, N.H., Ellis-Soto, D., Faxon, H.O., Goldstein, J.E., Halpern, B.S., Longdon, J., Norman, K.E.A., O'Rourke, D., Scoville, C., Xu, L., Boettiger, C., 2024. Biodiversity monitoring for a just planetary future. Science 383, 34–36. https://doi.org/10.1126/science.adh8874

Chazdon, R.L., Blüthgen, N., Brancalion, P.H.S., Heinrich, V., Bongers, F., 2025. Drivers and benefits of natural regeneration in tropical forests. Nat. Rev. Biodivers. 1, 298–314. https://doi.org/10.1038/s44358-025-00043-y

Chazdon, R.L., Falk, D.A., Banin, L.F., Wagner, M., Wilson, S.J., Grabowski, R.C., Suding, K.N., 2024. The intervention continuum in restoration ecology: rethinking the active–passive dichotomy. Restoration Ecology 32, e13535. https://doi.org/10.1111/rec.13535

Cole, R.J., Werden, L.K., Arroyo, F.C., Quirós, K.M., Cedeño, G.Q., Crowther, T.W., 2024. Forest restoration in practice across Latin America. Biological Conservation 294, 110608. https://doi.org/10.1016/j.biocon.2024.110608

Cooper, D.L.M., Lewis, S.L., Sullivan, M.J.P., Prado, P.I., ter Steege, H., Barbier, N., Slik, F., Sonké, B., Ewango, C.E.N., Adu-Bredu, S., Affum-Baffoe, K., de Aguiar, D.P.P., Ahuite Reategui, M.A., Aiba, S.-I., Albuquerque, B.W., de Almeida Matos, F.D., Alonso, A., Amani, C.A., do Amaral, D.D., do Amaral, I.L., Andrade, A., de Andrade Miranda, I.P., Angoboy, I.B., Araujo-Murakami, A., Arboleda, N.C., Arroyo, L., Ashton, P., Aymard C, G.A., Baider, C., Baker, T.R., Balinga, M.P.B., Balslev, H., Banin, L.F., Bánki, O.S., Baraloto, C., Barbosa, E.M., Barbosa, F.R., Barlow, J., Bastin, J.-F., Beeckman, H., Begne, S., Bengone, N.N., Berenguer, E., Berry, N., Bitariho, R., Boeckx, P., Bogaert, J., Bonyoma, B., Boundja, P., Bourland, N., Boyemba Bosela, F., Brambach, F., Brienen, R., Burslem, D.F.R.P., Camargo, J.L., Campelo, W., Cano, A., Cárdenas, S., Cárdenas López, D., de Sá Carpanedo, R., Carrero Márquez, Y.A., Carvalho, F.A., Casas, L.F., Castellanos, H., Castilho, C.V., Cerón, C., Chapman, C.A., Chave, J., Chhang, P., Chutipong, W., Chuyong, G.B., Cintra, B.B.L., Clark, C.J., Coelho de Souza, F., Comiskey, J.A., Coomes, D.A., Cornejo Valverde, F., Correa, D.F., Costa, F.R.C., Costa, J.B.P., Couteron, P., Culmsee, H., Cuni-Sanchez, A.,

Dallmeier, F., Damasco, G., Dauby, G., Dávila, N., Dávila Doza, H.P., De Alban, J.D.T., de Assis, R.L., De Canniere, C., De Haulleville, T., de Jesus Veiga Carim, M., Demarchi, L.O., Dexter, K.G., Di Fiore, A., Din, H.H.M., Disney, M.I., Djiofack, B.Y., Djuikouo, M.-N.K., Do, T.V., Doucet, J.-L., Draper, F.C., Droissart, V., Duivenvoorden, J.F., Engel, J., Estienne, V., Farfan-Rios, W., Fauset, S., Feeley, K.J., Feitosa, Y.O., Feldpausch, T.R., Ferreira, C., Ferreira, J., Ferreira, L.V., Fletcher, C.D., Flores, B.M., Fofanah, A., Foli, E.G., Fonty, É., Fredriksson, G.M., Fuentes, A., Galbraith, D., Gallardo Gonzales, G.P., Garcia-Cabrera, K., García-Villacorta, R., Gomes, V.H.F., Gómez, R.Z., Gonzales, T., Gribel, R., Guedes, M.C., Guevara, J.E., Hakeem, K.R., Hall, J.S., Hamer, K.C., Hamilton, A.C., Harris, D.J., Harrison, R.D., Hart, T.B., Hector, A., Henkel, T.W., Herbohn, J., Hockemba, M.B.N., Hoffman, B., Holmgren, M., Honorio Coronado, E.N., Huamantupa-Chuquimaco, I., Hubau, W., Imai, N., Irume, M.V., Jansen, P.A., Jeffery, K.J., Jimenez, E.M., Jucker, T., Junqueira, A.B., Kalamandeen, M., Kamdem, N.G., Kartawinata, K., Kasongo Yakusu, E., Katembo, J.M., Kearsley, E., Kenfack, D., Kessler, M., Khaing, T.T., Killeen, T.J., Kitayama, K., Klitgaard, B., Labrière, N., Laumonier, Y., Laurance, S.G.W., Laurance, W.F., Laurent, F., Le, T.C., Le, T.T., Leal, M.E., Leão de Moraes Novo, E.M., Levesley, A., Libalah, M.B., Licona, J.C., Lima Filho, D. de A., Lindsell, J.A., Lopes, A., Lopes, M.A., Lovett, J.C., Lowe, R., Lozada, J.R., Lu, X., Luambua, N.K., Luize, B.G., Maas, P., Magalhães, J.L.L., Magnusson, W.E., Mahayani, N.P.D., Makana, J.-R., Malhi, Y., Maniguaje Rincón, L., Mansor, A., Manzatto, A.G., Marimon, B.S., Marimon-Junior, B.H., Marshall, A.R., Martins, M.P., Mbayu, F.M., de Medeiros, M.B., Mesones, I., Metali, F., Mihindou, V., Millet, J., Milliken, W., Mogollón, H.F., Molino, J.-F., Mohd. Said, M.N., Monteagudo Mendoza, A., Montero, J.C., Moore, S., Mostacedo, B., Mozombite Pinto, L.F., Mukul, S.A., Munishi, P.K.T., Nagamasu, H., Nascimento, H.E.M., Nascimento, M.T., Neill, D., Nilus, R., Noronha, J.C., Nsenga, L., Núñez Vargas, P., Ojo, L., Oliveira, A.A., de Oliveira, E.A., Ondo, F.E., Palacios Cuenca, W., Pansini, S., Pansonato, M.P., Paredes, M.R., Paudel, E., Pauletto, D., Pearson, R.G., Pena, J.L.M., Pennington, R.T., Peres, C.A., Permana, A., Petronelli, P., Peñuela Mora, M.C., Phillips, J.F., Phillips, O.L., Pickavance, G., Piedade, M.T.F., Pitman, N.C.A., Ploton, P., Popelier, A., Poulsen, J.R., Prieto, A., Primack, R.B., Priyadi, H., Qie, L., Quaresma, A.C., de Queiroz, H.L., Ramirez-Angulo, H., Ramos, J.F., Reis, N.F.C., Reitsma, J., Revilla, J.D.C., Riutta, T., Rivas-Torres, G., Robiansyah, I., Rocha, M., Rodrigues, D. de J., Rodriguez-Ronderos, M.E., Rovero, F., Rozak, A.H., Rudas, A., Rutishauser, E., Sabatier, D., Sagang, L.B., Sampaio, A.F., Samsoedin, I., Satdichanh, M., Schietti, J., Schöngart, J., Scudeller, V.V., Seuaturien, N., Sheil, D., Sierra, R., Silman, M.R., Silva, T.S.F., da Silva Guimarães, J.R., Simo-Droissart, M., Simon, M.F., Sist, P., Sousa, T.R., de Sousa Farias, E., de Souza Coelho, L., Spracklen, D.V., Stas, S.M., Steinmetz, R., Stevenson, P.R., Stropp, J., Sukri, R.S., Sunderland, T.C.H., Suzuki, E., Swaine, M.D., Tang, J., Taplin, J., Taylor, D.M., Tello, J.S., Terborgh, J., Texier, N., Theilade, I., Thomas, D.W., Thomas, R., Thomas, S.C., Tirado, M., Toirambe, B., de Toledo, J.J., Tomlinson, K.W., Torres-Lezama, A., Tran, H.D., Tshibamba Mukendi, J., Tumaneng, R.D., Umaña, M.N., Umunay, P.M., Urrego Giraldo, L.E., Valderrama Sandoval, E.H., Valenzuela Gamarra, L., Van Andel, T.R., van de Bult, M., van de Pol, J., van der Heijden, G., Vasquez, R., Vela, C.I.A., Venticinque, E.M., Verbeeck, H., Veridiano, R.K.A., Vicentini, A., Vieira, I.C.G., Vilanova Torre, E., Villarroel, D., Villa Zegarra, B.E., Vleminckx, J., von Hildebrand, P., Vos, V.A., Vriesendorp, C., Webb, E.L., White, L.J.T., Wich, S., Wittmann, F., Zagt, R., Zang, R., Zartman, C.E., Zemagho, L., Zent, E.L., Zent, S., 2024. Consistent patterns of common species across tropical tree communities. Nature 625, 728–734. https://doi.org/10.1038/s41586-023-06820-z

costarica-sentinel-2-l2-spectral-indices [WWW Document], n.d. . Theia-Mtp STAC Browser. URL https://api.stac.teledetection.fr (accessed 9.10.25).

Crowe, O., Beresford, A.E., Buchanan, G.M., Grantham, H.S., Simkins, A.T., Watson, J.E.M., Butchart, S.H.M., 2023. A global assessment of forest integrity within Key Biodiversity Areas. Biological Conservation 286, 110293. https://doi.org/10.1016/j.biocon.2023.110293

Curtis, P.G., Slay, C.M., Harris, N.L., Tyukavina, A., Hansen, M.C., 2018. Classifying drivers of global forest loss. Science 361, 1108–1111. https://doi.org/10.1126/science.aau3445

Dias, A., Van Houdt, S., Meschin, K., Von Stackelberg, K., Bago, M.-L., Baldarelli, L., Gonzalez Downs, K., Luuk, M., Delubac, T., Bottagisio, E., Kasak, K., Kebabci, A., Levers, O., Miilvee, I., Paju-Hamburg, J., Poncet, R., Sanfilippo, M., Sildam, J., Stepanov, D., Karnauskaite, D., 2023. Using essential biodiversity variables to assess forest ecosystem integrity. Front. For. Glob. Change 6. https://doi.org/10.3389/ffgc.2023.1098901

Edgar, G.J., 2025. IUCN Red List criteria fail to recognise most threatened and extinct species. Biological Conservation 301, 110880. https://doi.org/10.1016/j.biocon.2024.110880

Fahrig, L., 2017. Ecological Responses to Habitat Fragmentation Per Se. Annual Review of Ecology, Evolution, and Systematics 48, 1–23. https://doi.org/10.1146/annurev-ecolsys-110316-022612

Fahrig, L., 2013. Rethinking patch size and isolation effects: the habitat amount hypothesis. Journal of Biogeography 40, 1649–1663. https://doi.org/10.1111/jbi.12130

FAO, 2025. Global Forest Resources Assessment 2025 [WWW Document]. Global Forest Resources Assessment. https://doi.org/10.4060/cd6709en

Fernández, N., Ferrier, S., Navarro, L.M., Pereira, H.M., 2020. Essential Biodiversity Variables: Integrating In-Situ Observations and Remote Sensing Through Modeling, in: Cavender-Bares, J., Gamon, J.A., Townsend, P.A. (Eds.), Remote Sensing of Plant Biodiversity. Springer International Publishing, Cham, pp. 485–501. https://doi.org/10.1007/978-3-030-33157-3_18

Fung, E., Imbach, P., Corrales, L., Vilchez, S., Zamora, N., Argotty, F., Hannah, L., Ramos, Z., 2017. Mapping conservation priorities and connectivity pathways under climate change for tropical ecosystems. Climatic Change 141, 77–92.

GBIF.org, 2025a. GBIF Occurrence Download [WWW Document]. URL https://www.gbif.org/occurrence/download/0000097-250227125302545 (accessed 2.24.26).

GBIF.org, 2025b. GBIF Occurrence Download [WWW Document]. URL https://www.gbif.org/occurrence/download/0000840-250226211518916 (accessed 2.24.26).

GBIF.org, 2025c. GBIF Occurrence Download [WWW Document]. URL https://www.gbif.org/occurrence/download/0000086-250227125302545 (accessed 2.24.26).

GBIF.org, 2025d. GBIF Occurrence Download [WWW Document]. URL https://www.gbif.org/occurrence/download/0000794-250226211518916 (accessed 2.24.26).

GBIF.org, 2025e. GBIF Occurrence Download [WWW Document]. URL https://www.gbif.org/occurrence/download/0000082-250227125302545 (accessed 2.24.26).

GBIF.org, 2025f. GBIF Occurrence Download [WWW Document]. URL https://www.gbif.org/occurrence/download/0000821-250226211518916 (accessed 2.24.26).

GBIF.org, 2025g. GBIF Occurrence Download [WWW Document]. URL https://www.gbif.org/occurrence/download/0000815-250226211518916 (accessed 2.24.26).

GBIF.org, 2025h. GBIF Occurrence Download [WWW Document]. URL https://www.gbif.org/occurrence/download/0000813-250226211518916 (accessed 2.24.26).

GBIF.org, 2025i. GBIF Occurrence Download [WWW Document]. URL https://www.gbif.org/occurrence/download/0000064-250227125302545 (accessed 2.24.26).

GBIF.org, 2025j. GBIF Occurrence Download [WWW Document]. URL https://www.gbif.org/occurrence/download/0000060-250227125302545 (accessed 2.24.26).

Unit, B., 2024. Consolidated Target Guidance Notes [WWW Document]. URL https://www.cbd.int/gbf/targets/notes.shtml (accessed 7.21.26).

Gibson, L., Lee, T.M., Koh, L.P., Brook, B.W., Gardner, T.A., Barlow, J., Peres, C.A., Bradshaw, C.J.A., Laurance, W.F., Lovejoy, T.E., Sodhi, N.S., 2011. Primary forests are irreplaceable for sustaining tropical biodiversity. Nature 478, 378–381. https://doi.org/10.1038/nature10425

Gilbert, L., Kappelle, M., 2016. The Southern Pacific Lowland Evergreen Moist Forest of the Osa Region, in: Costa Rican Ecosystems. The University of Chicago Press, M.Kappelle, pp. 360–411.

Grantham, H.S., Duncan, A., Evans, T.D., Jones, K.R., Beyer, H.L., Schuster, R., Walston, J., Ray, J.C., Robinson, J.G., Callow, M., Clements, T., Costa, H.M., DeGemmis, A., Elsen, P.R., Ervin, J., Franco, P., Goldman, E., Goetz, S., Hansen, A., Hofsvang, E., Jantz, P., Jupiter, S., Kang, A., Langhammer, P., Laurance, W.F., Lieberman, S., Linkie, M., Malhi, Y., Maxwell, S., Mendez, M., Mittermeier, R., Murray, N.J., Possingham, H., Radachowsky, J., Saatchi, S., Samper, C., Silverman, J., Shapiro, A., Strassburg, B., Stevens, T., Stokes, E., Taylor, R., Tear, T., Tizard, R., Venter, O., Visconti, P., Wang, S., Watson, J.E.M., 2020. Anthropogenic modification of forests means only 40% of remaining forests have high ecosystem integrity. Nat Commun 11, 5978. https://doi.org/10.1038/s41467-020-19493-3

Guisan, A., Tingley, R., Baumgartner, J.B., Naujokaitis-Lewis, I., Sutcliffe, P.R., Tulloch, A.I.T., Regan, T.J., Brotons, L., McDonald-Madden, E., Mantyka-Pringle, C., Martin, T.G., Rhodes, J.R., Maggini, R., Setterfield, S.A., Elith, J., Schwartz, M.W., Wintle, B.A., Broennimann, O., Austin, M., Ferrier, S., Kearney, M.R., Possingham, H.P., Buckley, Y.M., 2013. Predicting species distributions for conservation decisions. Ecology Letters 16, 1424–1435. https://doi.org/10.1111/ele.12189

Haddad, N.M., Brudvig, L.A., Clobert, J., Davies, K.F., Gonzalez, A., Holt, R.D., Lovejoy, T.E., Sexton, J.O., Austin, M.P., Collins, C.D., Cook, W.M., Damschen, E.I., Ewers, R.M., Foster, B.L., Jenkins, C.N., King, A.J., Laurance, W.F., Levey, D.J., Margules, C.R., Melbourne, B.A., Nicholls, A.O., Orrock, J.L., Song, D.-X., Townshend, J.R., 2015. Habitat fragmentation and its lasting impact on Earth's ecosystems. Science Advances. https://doi.org/10.1126/sciadv.1500052

Hagen-Zanker, A., 2016. A computational framework for generalized moving windows and its application to landscape pattern analysis. International Journal of Applied Earth Observation and Geoinformation 44, 205–216. https://doi.org/10.1016/j.jag.2015.09.010

Hanley, J.A., McNeil, B.J., 1982. The meaning and use of the area under a receiver operating characteristic (ROC) curve. Radiology 143, 29–36. https://doi.org/10.1148/radiology.143.1.7063747

Hanson, J.O., Schuster, R., Strimas-Mackey, M., Morrell, N., Edwards, B.P.M., Arcese, P., Bennett, J.R., Possingham, H.P., 2025. Systematic conservation prioritization with the prioritizr R package. Conservation Biology 39, e14376. https://doi.org/10.1111/cobi.14376

Hawkins, B.A., Leroy, B., Rodríguez, M.Á., Singer, A., Vilela, B., Villalobos, F., Wang, X., Zelený, D., 2017. Structural bias in aggregated species-level variables driven by repeated species co-occurrences: a pervasive problem in community and assemblage data. Journal of Biogeography 44, 1199–1211. https://doi.org/10.1111/jbi.12953

Hengl, T., Jesus, J.M. de, Heuvelink, G.B.M., Gonzalez, M.R., Kilibarda, M., Blagotić, A., Shangguan, W., Wright, M.N., Geng, X., Bauer-Marschallinger, B., Guevara, M.A., Vargas, R., MacMillan, R.A., Batjes, N.H., Leenaars, J.G.B., Ribeiro, E., Wheeler, I., Mantel, S., Kempen, B., 2017. SoilGrids250m: Global

gridded soil information based on machine learning. PLOS ONE 12, e0169748. https://doi.org/10.1371/journal.pone.0169748

Hesselbarth, M.H.K., Sciaini, M., With, K.A., Wiegand, K., Nowosad, J., 2019. landscapemetrics : an open-source R tool to calculate landscape metrics. Ecography 42, 1648–1657. https://doi.org/10.1111/ecog.04617

Hofhansl, F., Chacón-Madrigal, E., Morera, A., Huber, W., Weissenhofer, A., Wanek, W., 2019. Diversity and composition of tropical forest plant communities in the Golfo Dulce region.

Holl, K.D., Luong, J.C., Brancalion, P.H.S., 2022. Overcoming biotic homogenization in ecological restoration. Trends in Ecology & Evolution 37, 777–788. https://doi.org/10.1016/j.tree.2022.05.002

Hughes, A.C., Grumbine, R.E., 2023. The Kunming-Montreal Global Biodiversity Framework: what it does and does not do, and how to improve it. Front. Environ. Sci. 11. https://doi.org/10.3389/fenvs.2023.1281536

IUCN, 2016. A Global Standard for the Identification of Key Biodiversity Areas.

Jones, K.R., Venter, O., Fuller, R.A., Allan, J.R., Maxwell, S.L., Negret, P.J., Watson, J.E.M., 2018. One-third of global protected land is under intense human pressure. Science 360, 788–791. https://doi.org/10.1126/science.aap9565

Kaky, E., Nolan, V., Alatawi, A., Gilbert, F., 2020. A comparison between Ensemble and MaxEnt species distribution modelling approaches for conservation: A case study with Egyptian medicinal plants. Ecological Informatics 60, 101150. https://doi.org/10.1016/j.ecoinf.2020.101150

Karger, D.N., Conrad, O., Böhner, J., Kawohl, T., Kreft, H., Soria-Auza, R.W., Zimmermann, N.E., Linder, H.P., Kessler, M., 2017. Climatologies at high resolution for the earth's land surface areas. Sci Data 4, 170122. https://doi.org/10.1038/sdata.2017.122

Keppel, G., Mokany, K., Wardell-Johnson, G.W., Phillips, B.L., Welbergen, J.A., Reside, A.E., 2015. The capacity of refugia for conservation planning under climate change. Frontiers in Ecology and the Environment 13, 106–112. https://doi.org/10.1890/140055

Keppel, G., Niel, K.P.V., Wardell-Johnson, G.W., Yates, C.J., Byrne, M., Mucina, L., Schut, A.G.T., Hopper, S.D., Franklin, S.E., 2012. Refugia: identifying and understanding safe havens for biodiversity under climate change. Global Ecology and Biogeography 21, 393–404. https://doi.org/10.1111/j.1466-8238.2011.00686.x

Kohlmann, B., Roderus, D., Elle, O., Solís, Á., Soto, X., Russo, R., 2010. Biodiversity conservation in Costa Rica: a correspondence analysis between identified biodiversity hotspots (Araceae, Arecaceae, Bromeliaceae, and Scarabaeinae) and conservation priority life zones. Revista mexicana de biodiversidad 81, 511–559.

Konowalik, K., Nosol, A., 2021. Evaluation metrics and validation of presence-only species distribution models based on distributional maps with varying coverage. Sci Rep 11, 1482. https://doi.org/10.1038/s41598-020-80062-1

Lima, R.B. de, Silva, D.A.S. da, Nunes, M.H., Bittencourt, P.R. de L., Groenendyk, P., Oliveira, C.P. de, Granato-Souza, D., Ferreira, R.L.C., Silva, J.A.A. da, Aguirre-Gutiérrez, J., Jackson, T., Filho, J.R. de M., Aparício, P. da S., Silva, J.P.G. da, Toledo, J.J. de, Guedes, M.C., Almeida, D.R.A. de, Higuchi, N., Wagner, F.H., Ometto, J.P., Görgens, E.B., 2026. Mapping the density of giant trees in the Amazon. New Phytologist 249, 152–168. https://doi.org/10.1111/nph.70634

Lindenmayer, D., Pierson, J., Barton, P., Beger, M., Branquinho, C., Calhoun, A., Caro, T., Greig, H., Gross, J., Heino, J., Hunter, M., Lane, P., Longo, C., Martin, K., McDowell, W.H., Mellin, C., Salo, H., Tulloch, A., Westgate, M., 2015. A new framework for selecting environmental surrogates. Science of The Total Environment 538, 1029–1038. https://doi.org/10.1016/j.scitotenv.2015.08.056

Lohbeck, M., Bongers, F., Martinez-Ramos, M., Poorter, L., 2016. The importance of biodiversity and dominance for multiple ecosystem functions in a human-modified tropical landscape. Ecology 97, 2772–2779. https://doi.org/10.1002/ecy.1499

Louail, T., Lenormand, M., Cantu Ros, O.G., Picornell, M., Herranz, R., Frias-Martinez, E., Ramasco, J.J., Barthelemy, M., 2014. From mobile phone data to the spatial structure of cities. Sci Rep 4, 5276. https://doi.org/10.1038/srep05276

Marshall, A.R., Waite, C.E., Pfeifer, M., Banin, L.F., Rakotonarivo, S., Chomba, S., Herbohn, J., Gilmour, D.A., Brown, M., Chazdon, R.L., 2022. Fifteen essential science advances needed for effective restoration of the world's forest landscapes. Philos Trans R Soc Lond B Biol Sci 378, 20210065. https://doi.org/10.1098/rstb.2021.0065

Martini, F., Kounnamas, C., Goodale, E., Mammides, C., 2024. Examining the co-occurrences of human threats within terrestrial protected areas. Ambio 53, 592–603. https://doi.org/10.1007/s13280-023-01966-6

McCullough, I.M., Beirne, C., Soto-Navarro, C., Whitworth, A., 2024. Mapping climate adaptation corridors for biodiversity—A regional-scale case study in Central America. PLOS ONE 19, e0304756. https://doi.org/10.1371/journal.pone.0304756

McGarigal, K., Cushman, S.A., Ene, E., 2022. FRAGSTATS v4: Spatial Pattern Analysis Program for Categorical Maps.

Metcalfe, D.B., Anders, E., Axén, H., Petter Axelsson, E., Bermudez, A.E., Bartholomew, D.C., Butt, N., Cadillo-Quiroz, H., Chaudhary, N., Callebaut, T., Dahlsjö, C.A.L., Dusenge, M.E., Feeley, K.J., Wanger, T.C., Hwang, B.C., Hermans, T.D.G., Jonsson, M., Kardol, P., Lindh, A., Lussetti, D., Lamba, S., Mewett, G., Mujawamariya, M., Manzi, O.J.L., Salinas, N., Prevéy, J.S., Bargués-Tobella, A., Tang, J., Vought, O.K., Witteman, M., Wallin, G., Zhang, W., Yan, Y., Virkkala, A.-M., 2025. Gaps in tropical science from unrepresentative distribution of sampling and citation across natural terrestrial environments. Nat Commun 16, 11378. https://doi.org/10.1038/s41467-025-67617-4

MINAE, 2015. Política nacional de biodiversidad 2015-2030 Costa Rica.

MINAE, 1996. Ley Forestal N°7575.

Montero, A., Marull, J., Tello, E., Cattaneo, C., Coll, F., Pons, M., Infante-Amate, J., Urrego-Mesa, A., Fernández-Landa, A., Vargas, M., 2021. The impacts of agricultural and urban land-use changes on plant and bird biodiversity in Costa Rica (1986–2014). Reg Environ Change 21, 48. https://doi.org/10.1007/s10113-021-01767-1

Montoya-Jiménez, J.C., Valdez-Lazalde, J.R., Ángeles-Perez, G., De Los Santos-Posadas, H.M., Cruz-Cárdenas, G., 2022. Predictive capacity of nine algorithms and an ensemble model to determine the geographic distribution of tree species. iForest - Biogeosciences and Forestry 15, 363. https://doi.org/10.3832/ifor4084-015

Morera Beita, C., Murillo, L.F.S., Alvarado, L.D.A., 2021. Ecological corridors in Costa Rica: An evaluation applying landscape structure, fragmentation-connectivity process, and climate adaptation. Conservat Sci and Prac 3. https://doi.org/10.1111/csp2.475

Mrema, E.M., Crowther, T.W., Mathai, W., Brooks, T., Archibald, S., Brancalion, P., Barbier, E.B., Obura, D., Reyes-García, V., Bond, W.J., Koh, L.P., Christophersen, T., Brondizio, E.S., 2020. Ten years to restore a planet. One Earth 3, 647–652. https://doi.org/10.1016/j.oneear.2020.11.015

NASA JPL, 2020. NASADEM Merged DEM Global 1 arc second V001. https://doi.org/10.5067/MEASURES/NASADEM/NASADEM_HGT.001

Nunes, M.H., Vaz, M.C., Camargo, J.L.C., Laurance, W.F., de Andrade, A., Vicentini, A., Laurance, S., Raumonen, P., Jackson, T., Zuquim, G., Wu, J., Peñuelas, J., Chave, J., Maeda, E.E., 2023. Edge effects on tree architecture exacerbate biomass loss of fragmented Amazonian forests. Nat Commun 14, 8129. https://doi.org/10.1038/s41467-023-44004-5

Pendrill, F., Gardner, T.A., Meyfroidt, P., Persson, U.M., Adams, J., Azevedo, T., Bastos Lima, M.G., Baumann, M., Curtis, P.G., De Sy, V., Garrett, R., Godar, J., Goldman, E.D., Hansen, M.C., Heilmayr, R., Herold, M., Kuemmerle, T., Lathuillière, M.J., Ribeiro, V., Tyukavina, A., Weisse, M.J., West, C., 2022. Disentangling the numbers behind agriculture-driven tropical deforestation. Science 377, eabm9267. https://doi.org/10.1126/science.abm9267

Pla, M., Hermoso, V., Pino, J., Brotons, L., 2024. Mapping pressures on biodiversity: the contribution of thematic detail to decision making. Biodivers Conserv 33, 1079–1098. https://doi.org/10.1007/s10531-024-02786-0

Plumptre, A., Hayes, J., Baisero, D., Rose, R., Holness, S., von Staden, L., Smith, R.J., 2025. Strengths and complementarity of systematic conservation planning and Key Biodiversity Area approaches for spatial planning. Conservation Biology 39, e14400. https://doi.org/10.1111/cobi.14400

Possingham, H.P., Bode, M., Klein, C.J., 2015. Optimal Conservation Outcomes Require Both Restoration and Protection. PLOS Biology 13, e1002052. https://doi.org/10.1371/journal.pbio.1002052

Préau, C., Dubos, N., Lenormand, M., Denelle, P., Le Louarn, M., Alleaume, S., Luque, S., 2022. Dispersal-based species pools as sources of connectivity area mismatches. Landsc Ecol 37, 729–743. https://doi.org/10.1007/s10980-021-01371-y

R Core Team, 2024. R: The R Project for Statistical Computing [WWW Document]. URL https://www.r-project.org/ (accessed 12.20.24).

Redo, D.J., Grau, H.R., Aide, T.M., Clark, M.L., 2012. Asymmetric forest transition driven by the interaction of socioeconomic development and environmental heterogeneity in Central America. Proc. Natl. Acad. Sci. U.S.A. 109, 8839–8844. https://doi.org/10.1073/pnas.1201664109

Rey, P.-L., Martin, C., Guisan, A., 2024. Conservation importance of non-threatened species through their direct linkages with nature's contributions to people. Biological Conservation 297, 110733. https://doi.org/10.1016/j.biocon.2024.110733

Ritter, C.D., Faurby, S., Bennett, D.J., Naka, L.N., ter Steege, H., Zizka, A., Haenel, Q., Nilsson, R.H., Antonelli, A., 2019. The pitfalls of biodiversity proxies: Differences in richness patterns of birds, trees and understudied diversity across Amazonia. Sci Rep 9, 19205. https://doi.org/10.1038/s41598-019-55490-3

Rosenfield, M.F., Jakovac, C.C., Vieira, D.L.M., Poorter, L., Brancalion, P.H.S., Vieira, I.C.G., de Almeida, D.R.A., Massoca, P., Schietti, J., Albernaz, A.L.M., Ferreira, M.J., Mesquita, R.C.G., 2023. Ecological integrity of tropical secondary forests: concepts and indicators. Biological Reviews 98, 662–676. https://doi.org/10.1111/brv.12924

Rüger, N., Schorn, M.E., Kambach, S., Chazdon, R.L., Farrior, C.E., Meave, J.A., Muñoz, R., Van Breugel, M., Amissah, L., Bongers, F., Craven, D., Hérault, B., Jakovac, C.C., Norden, N., Poorter, L., Van Der Sande, M.T., Wirth, C., Delgado, D., Dent, D.H., DeWalt, S.J., Dupuy, J.M., Finegan, B., Hall, J.S., Hernández-Stefanoni, J.L., Lopez, O.R., 2023. Successional shifts in tree demographic strategies in wet and dry Neotropical forests. Global Ecol Biogeogr 32, 1002–1014. https://doi.org/10.1111/geb.13669

Salom-Pérez, R., Corrales-Gutiérrez, D., Araya-Gamboa, D., Espinoza-Muñoz, D., Finegan, B., Petracca, L.S., 2021. Forest cover mediates large and medium-sized mammal occurrence in a critical link of the Mesoamerican Biological Corridor. PLOS ONE 16, e0249072. https://doi.org/10.1371/journal.pone.0249072

Sampaio, A.C.P., Cavalcante, A.D.M.B., 2023. Accurate species distribution models: minimum required number of specimen records in the Caatinga biome. An. Acad. Bras. Ciênc. 95, e20201421. https://doi.org/https://doi.org/10.1590/0001-3765202320201421

Saura, S., Bertzky, B., Bastin, L., Battistella, L., Mandrici, A., Dubois, G., 2018. Protected area connectivity: Shortfalls in global targets and country-level priorities. Biological Conservation 219, 53–67. https://doi.org/10.1016/j.biocon.2017.12.020

Schmitt, S., Pouteau, R., Justeau, D., de Boissieu, F., Birnbaum, P., 2017. ssdm: An r package to predict distribution of species richness and composition based on stacked species distribution models. Methods in Ecology and Evolution 8, 1795–1803. https://doi.org/10.1111/2041-210X.12841

Selwood, K.E., Zimmer, H.C., 2020. Refuges for biodiversity conservation: A review of the evidence. Biological Conservation 245, 108502. https://doi.org/10.1016/j.biocon.2020.108502

Shaver, I., Chain-Guadarrama, A., Cleary, K.A., Sanfiorenzo, A., Santiago-García, R.J., Finegan, B., Hormel, L., Sibelet, N., Vierling, L.A., Bosque-Pérez, N.A., DeClerck, F., Fagan, M.E., Waits, L.P., 2015. Coupled social and ecological outcomes of agricultural intensification in Costa Rica and the future of biodiversity conservation in tropical agricultural regions. Global Environmental Change 32, 74–86. https://doi.org/10.1016/j.gloenvcha.2015.02.006

Shrestha, N., Xu, X., Meng, J., Wang, Z., 2021. Vulnerabilities of protected lands in the face of climate and human footprint changes. Nat Commun 12, 1632. https://doi.org/10.1038/s41467-021-21914-w

Šímová, P., Gdulová, K., 2012. Landscape indices behavior: A review of scale effects. Applied Geography 34, 385–394. https://doi.org/10.1016/j.apgeog.2012.01.003

SINAC, 2021. Mapa de tipos de Bosque y otras tierras de Costa Rica 2021 [WWW Document]. URL https://www.sinac.go.cr/ES/bimapas/Paginas/mabosq2021.aspx (accessed 2.25.25).

SINAC, n.d. Programa Nacional de Corredores Biológicos (PNCB) [WWW Document]. URL https://sinac.go.cr/ES/partciudygober/Paginas/pncb.aspx (accessed 2.28.26).

SNIT [WWW Document], n.d. URL https://www.snitcr.go.cr/ico_servicios_ogc_info?k=bm9kbzo6NDA=&nombre=SINAC (accessed 9.10.25).

Souza Oliveira, M., Lenormand, M., Luque, S., Zamora, N.A., Alleaume, S., Aguilar Porras, A.C., Castillo, M.U., Chacón-Madrigal, E., Delgado, D., Hernández Sánchez, L.G., Ngo Bieng, M.-A., Quesada-Monge, R., Solano, G.S., Zúñiga, P.M., 2025a. Unlocking Tropical Forest Complexity: How Tree Assemblages in Secondary Forests Boost Biodiversity Conservation. Ecology and Evolution 15, e72428. https://doi.org/10.1002/ece3.72428

Souza Oliveira, M., Préau, C., Alleaume, S., Lenormand, M., Luque, S., 2025b. Modelling species distributions using remote sensing predictors: Comparing dynamic habitat index and LULC. Ecological Indicators 179, 114198. https://doi.org/10.1016/j.ecolind.2025.114198

Strassburg, B.B.N., Iribarrem, A., Beyer, H.L., Cordeiro, C.L., Crouzeilles, R., Jakovac, C.C., Braga Junqueira, A., Lacerda, E., Latawiec, A.E., Balmford, A., Brooks, T.M., Butchart, S.H.M., Chazdon, R.L., Erb, K.-H., Brancalion, P., Buchanan, G., Cooper, D., Díaz, S., Donald, P.F., Kapos, V., Leclère, D., Miles, L., Obersteiner, M., Plutzar, C., de M. Scaramuzza, C.A., Scarano, F.R., Visconti, P., 2020. Global priority areas for ecosystem restoration. Nature 586, 724–729. https://doi.org/10.1038/s41586-020-2784-9

ter Steege, H., Pitman, N.C.A., do Amaral, I.L., de Souza Coelho, L., de Almeida Matos, F.D., de Andrade Lima Filho, D., Salomão, R.P., Wittmann, F., Castilho, C.V., Guevara, J.E., Veiga Carim, M. de J., Phillips, O.L., Magnusson, W.E., Sabatier, D., Revilla, J.D.C., Molino, J.-F., Irume, M.V., Martins, M.P., da Silva Guimarães, J.R., Ramos, J.F., Bánki, O.S., Piedade, M.T.F., Cárdenas López, D., Rodrigues, D. de J., Demarchi, L.O., Schöngart, J., Almeida, E.J., Barbosa, L.F., Cavalheiro, L., dos Santos, M.C.V., Luize, B.G., de Leão Novo, E.M.M., Vargas, P.N., Silva, T.S.F., Venticinque, E.M., Manzatto, A.G., Reis, N.F.C., Terborgh, J., Casula, K.R., Honorio Coronado, E.N., Monteagudo Mendoza, A., Montero, J.C., Costa, F.R.C., Feldpausch, T.R., Quaresma, A.C., Castaño Arboleda, N., Zartman, C.E., Killeen, T.J., Marimon, B.S., Marimon-Junior, B.H., Vasquez, R., Mostacedo, B., Assis, R.L., Baraloto, C., do Amaral, D.D., Engel, J., Petronelli, P., Castellanos, H., de Medeiros, M.B., Simon, M.F., Andrade, A., Camargo, J.L., Laurance, W.F., Laurance, S.G.W., Maniguaje Rincón, L., Schietti, J., Sousa, T.R., de Sousa Farias, E., Lopes, M.A., Magalhães, J.L.L., Nascimento, H.E.M., de Queiroz, H.L., Aymard C., G.A., Brienen, R., Stevenson, P.R., Araujo-Murakami, A., Baker, T.R., Cintra, B.B.L., Feitosa, Y.O., Mogollón, H.F., Duivenvoorden, J.F., Peres, C.A., Silman, M.R., Ferreira, L.V., Lozada, J.R., Comiskey, J.A., Draper, F.C., de Toledo, J.J., Damasco, G., García-Villacorta, R., Lopes, A., Vicentini, A., Cornejo Valverde, F., Alonso, A., Arroyo, L., Dallmeier, F., Gomes, V.H.F., Jimenez, E.M., Neill, D., Peñuela Mora, M.C., Noronha, J.C., de Aguiar, D.P.P., Barbosa, F.R., Bredin, Y.K., de Sá Carpanedo, R., Carvalho, F.A., de Souza, F.C., Feeley, K.J., Gribel, R., Haugaasen, T., Hawes, J.E., Pansonato, M.P., Ríos Paredes, M., Barlow, J., Berenguer, E., da Silva, I.B., Ferreira, M.J., Ferreira, J., Fine, P.V.A., Guedes, M.C., Levis, C., Licona, J.C., Villa Zegarra, B.E., Vos, V.A., Cerón, C., Durgante, F.M., Fonty, É., Henkel, T.W., Householder, J.E., Huamantupa-Chuquimaco, I., Pos, E., Silveira, M., Stropp, J., Thomas, R., Daly, D., Dexter, K.G., Milliken, W., Molina, G.P., Pennington, T., Vieira, I.C.G., Weiss Albuquerque, B., Campelo, W., Fuentes, A., Klitgaard, B., Pena, J.L.M., Tello, J.S., Vriesendorp, C., Chave, J., Di Fiore, A., Hilário, R.R., de Oliveira Pereira, L., Phillips, J.F., Rivas-Torres, G., van Andel, T.R., von Hildebrand, P., Balee, W., Barbosa, E.M., de Matos Bonates, L.C., Dávila Doza, H.P., Zárate Gómez, R., Gonzales, T., Gallardo Gonzales, G.P., Hoffman, B., Junqueira, A.B., Malhi, Y., de Andrade Miranda, I.P., Pinto, L.F.M., Prieto, A., Rudas, A., Ruschel, A.R., Silva, N., Vela, C.I.A., Zent, E.L., Zent, S., Cano, A., Carrero Márquez, Y.A., Correa, D.F., Costa, J.B.P., Flores, B.M., Galbraith, D., Holmgren, M., Kalamandeen, M., Lobo, G., Torres Montenegro, L., Nascimento, M.T., Oliveira, A.A., Pombo, M.M., Ramirez-Angulo, H., Rocha, M., Scudeller, V.V., Sierra, R., Tirado, M., Umaña, M.N., van der Heijden, G., Vilanova Torre, E., Reategui, M.A.A., Baider, C., Balslev, H., Cárdenas, S., Casas, L.F., Endara, M.J., Farfan-Rios, W., Ferreira, C., Linares-Palomino, R., Mendoza, C., Mesones, I., Parada, G.A., Torres-Lezama, A., Urrego Giraldo, L.E., Villarroel, D., Zagt, R., Alexiades, M.N., de Oliveira, E.A., Garcia-Cabrera, K., Hernandez, L., Cuenca, W.P., Pansini, S., Pauletto, D., Ramirez Arevalo, F., Sampaio, A.F., Valderrama Sandoval, E.H., Gamarra, L.V., Levesley, A., Pickavance, G., Melgaço, K., 2023. Mapping density, diversity and species-richness of the Amazon tree flora. Commun Biol 6, 1130. https://doi.org/10.1038/s42003-023-05514-6

ter Steege, H., Pitman, N.C.A., Sabatier, D., Baraloto, C., Salomão, R.P., Guevara, J.E., Phillips, O.L., Castilho, C.V., Magnusson, W.E., Molino, J.-F., Monteagudo, A., Núñez Vargas, P., Montero, J.C., Feldpausch, T.R., Coronado, E.N.H., Killeen, T.J., Mostacedo, B., Vasquez, R., Assis, R.L., Terborgh, J.,

Wittmann, F., Andrade, A., Laurance, W.F., Laurance, S.G.W., Marimon, B.S., Marimon, B.-H., Guimarães Vieira, I.C., Amaral, I.L., Brienen, R., Castellanos, H., Cárdenas López, D., Duivenvoorden, J.F., Mogollón, H.F., Matos, F.D. de A., Dávila, N., García-Villacorta, R., Stevenson Diaz, P.R., Costa, F., Emilio, T., Levis, C., Schietti, J., Souza, P., Alonso, A., Dallmeier, F., Montoya, A.J.D., Fernandez Piedade, M.T., Araujo-Murakami, A., Arroyo, L., Gribel, R., Fine, P.V.A., Peres, C.A., Toledo, M., Aymard C., G.A., Baker, T.R., Cerón, C., Engel, J., Henkel, T.W., Maas, P., Petronelli, P., Stropp, J., Zartman, C.E., Daly, D., Neill, D., Silveira, M., Paredes, M.R., Chave, J., Lima Filho, D. de A., Jørgensen, P.M., Fuentes, A., Schöngart, J., Cornejo Valverde, F., Di Fiore, A., Jimenez, E.M., Peñuela Mora, M.C., Phillips, J.F., Rivas, G., van Andel, T.R., von Hildebrand, P., Hoffman, B., Zent, E.L., Malhi, Y., Prieto, A., Rudas, A., Ruschell, A.R., Silva, N., Vos, V., Zent, S., Oliveira, A.A., Schutz, A.C., Gonzales, T., Trindade Nascimento, M., Ramirez-Angulo, H., Sierra, R., Tirado, M., Umaña Medina, M.N., van der Heijden, G., Vela, C.I.A., Vilanova Torre, E., Vriesendorp, C., Wang, O., Young, K.R., Baider, C., Balslev, H., Ferreira, C., Mesones, I., Torres-Lezama, A., Urrego Giraldo, L.E., Zagt, R., Alexiades, M.N., Hernandez, L., Huamantupa-Chuquimaco, I., Milliken, W., Palacios Cuenca, W., Pauletto, D., Valderrama Sandoval, E., Valenzuela Gamarra, L., Dexter, K.G., Feeley, K., Lopez-Gonzalez, G., Silman, M.R., 2013. Hyperdominance in the Amazonian Tree Flora. Science 342, 1243092. https://doi.org/10.1126/science.1243092

Thomas, D.C., Ardi, W.H., Chong, Y.H., Thomas, P., Hughes, M., 2024. Conservation status assessments of species-rich tropical taxa in the face of data availability limitations: insights from Sulawesi Begonia. Sci Rep 14, 14007. https://doi.org/10.1038/s41598-024-64319-7

Thuiller, W., Guéguen, M., Renaud, J., Karger, D.N., Zimmermann, N.E., 2019. Uncertainty in ensembles of global biodiversity scenarios. Nat Commun 10, 1446. https://doi.org/10.1038/s41467-019-09519-w

Unit, B., 2024. Consolidated Target Guidance Notes [WWW Document]. URL https://www.cbd.int/gbf/targets/notes.shtml (accessed 7.21.26)

Vallé, C., Le Viol, I., Nabias, J., Princé, K., Gosselin, F., 2025. Tree species identity shapes the relationship between canopy cover and herb-layer species in temperate forests. Journal of Ecology 113, 582–597. https://doi.org/10.1111/1365-2745.14479

van Proosdij, A.S.J., Sosef, M.S.M., Wieringa, J.J., Raes, N., 2016. Minimum required number of specimen records to develop accurate species distribution models. Ecography 39, 542–552. https://doi.org/10.1111/ecog.01509

Ward, M., Saura, S., Williams, B., Ramírez-Delgado, J.P., Arafeh-Dalmau, N., Allan, J.R., Venter, O., Dubois, G., Watson, J.E.M., 2020. Just ten percent of the global terrestrial protected area network is structurally connected via intact land. Nat Commun 11, 4563. https://doi.org/10.1038/s41467-020-18457-x

Watson, J.E.M., Evans, T., Venter, O., Williams, B., Tulloch, A., Stewart, C., Thompson, I., Ray, J.C., Murray, K., Salazar, A., McAlpine, C., Potapov, P., Walston, J., Robinson, J.G., Painter, M., Wilkie, D., Filardi, C., Laurance, W.F., Houghton, R.A., Maxwell, S., Grantham, H., Samper, C., Wang, S., Laestadius, L., Runting, R.K., Silva-Chávez, G.A., Ervin, J., Lindenmayer, D., 2018. The exceptional value of intact forest ecosystems. Nat Ecol Evol 2, 599–610. https://doi.org/10.1038/s41559-018-0490-x

Yang, G., Crowther, T.W., Lauber, T., Zohner, C.M., Smith, G.R., 2025. A globally consistent negative effect of edge on aboveground forest biomass. Nat Ecol Evol 9, 2036–2045. https://doi.org/10.1038/s41559-025-02840-2

Zamora, N., Hammel, B.E., Grayum, M.H., 2004. Vegetation, in: Manual de Plantas de Costa Rica. Vol. I: Introducción. Monographs in Sys-tematic Botany from the Missouri Botanical Garden, pp. 91–216.

Zhang, S., Zang, R., Sheil, D., 2022. Rare and common species contribute disproportionately to the functional variation within tropical forests. Journal of Environmental Management 304, 114332. https://doi.org/10.1016/j.jenvman.2021.114332

Zizka, A., Carvalho, F.A., Calvente, A., Baez-Lizarazo, M.R., Cabral, A., Coelho, J.F.R., Colli-Silva, M., Fantinati, M.R., Fernandes, M.F., Ferreira-Araújo, T., Moreira, F.G.L., Santos, N.M.C., Santos, T.A.B., Santos-Costa, R.C. dos, Serrano, F.C., Silva, A.P.A. da, Soares, A. de S., Souza, P.G.C. de, Tomaz, E.C., Vale, V.F., Vieira, T.L., Antonelli, A., 2020. No one-size-fits-all solution to clean GBIF. PeerJ 8, e9916. https://doi.org/10.7717/peerj.9916

Zurell, D., Franklin, J., König, C., Bouchet, P.J., Dormann, C.F., Elith, J., Fandos, G., Feng, X., Guillera-Arroita, G., Guisan, A., Lahoz-Monfort, J.J., Leitão, P.J., Park, D.S., Peterson, A.T., Rapacciuolo, G., Schmatz, D.R., Schröder, B., Serra-Diaz, J.M., Thuiller, W., Yates, K.L., Zimmermann, N.E., Merow, C., 2020. A standard protocol for reporting species distribution models. Ecography 43, 1261–1277. https://doi.org/10.1111/ecog.04960

Zwiener, V.P., Alves, V.A., 2023. Community-level predictions in a megadiverse hotspot: comparison of stacked species distribution models to forest inventory data. J Plant Ecol 16, rtac099. https://doi.org/10.1093/jpe/rtac099

Supplementary material

Section S1. Cross-scale sensitivity analysis to select the moving-window size

Landscape metrics derived from categorical LULC maps are scale dependent, and moving-window ("focal") calculations are commonly used to represent spatial variation in landscape composition/configuration as continuous surfaces. Because the window size controls the observation scale, we performed a cross-scale sensitivity analysis across a set of candidate window sizes and retained the window that provided a good compromise between (i) preservation of local spatial variability, (ii) avoidance of excessive smoothing, and (iii) consistency across scales (Hagen-Zanker, 2016).

Let $m_w(x)$ denote the raster value of a given class-level landscape metric at pixel location x, computed using a square moving window of side length w pixels (odd integers). Let s=250m, the pixel size. Candidate windows were $w \in \{5,11,21,31,41\}$ pixels. For each metric m and each window size w, we computed three complementary indices: (i) spatial roughness, (ii) global variance, and (iii) inter-scale stability.

(i) Spatial roughness index (mean absolute central difference; "MACD roughness") – To quantify how rapidly the metric surface varies locally (and how this variation decreases as the window size increases), we computed a roughness index based on absolute central differences in the horizontal and vertical directions. For raster cell(i, j), define:

$\Delta_x(i,j) = |m_w(i,j+1) - m_w(i,j-1)|$,

$\Delta_y(i,j) = |m_w(i+1,j) - m_w(i-1,j)|$.

The spatial roughness index is then:

$$R_w = \frac{1}{2}(\Delta_x + \Delta_y)$$

where the overbar denotes the mean over all cells for which the required neighbours exist and are non-missing.

(ii) Global variance – Global variance was computed as the (non-missing) variance of raster cell values of m_w, to characterise how overall map variability changes with window size (Šímová and Gdulová, 2012).

(iii) Inter-scale stability – Inter-scale stability was measured as the Pearson correlation between metric surfaces obtained at two window sizes w, evaluated over the intersection of pixels with valid values in both rasters.

Table S1. Exploration of the occurrence data of the studied species: "GBIF abundance" representing the number of occurrences of the species in the study area included in the GBIF data and, "Abundance (res 250m)" indicating species abundance at a spatial resolution of 250 m with at least 10 occurrences.

Species	GBIF abundance	Abundance (res 250m)
Adelia triloba	42	13
Aegiphila anomala	10	0
Aiouea montana	12	0
Albizia adinocephala	51	23
Albizia niopoides	24	0
Alchornea costaricensis	29	11
Alchornea glandulosa	34	0
Alchornea latifolia	66	19
Alchorneopsis floribunda	20	0
Alfaroa costaricensis	57	19
Alnus acuminata	43	23
Amyris pinnata	40	10
Anacardium excelsum	77	46
Anaxagorea crassipetala	46	15
Andira inermis	61	31
Annona montana	11	0
Annona papilionella	14	0
Annona purpurea	26	17
Apeiba membranacea	86	58
Apeiba tibourbou	138	98
Aralia excelsa	27	0
Ardisia compressa	115	48
Ardisia palmana	38	15
Ardisia pleurobotrya	41	0
Ardisia revoluta	53	26
Astronium graveolens	34	17
Axinaea costaricensis	11	0
Batocarpus costaricensis	17	0
Beilschmiedia costaricensis	14	0
Billia rosea	145	45
Bravaisia integerrima	22	12

Species	GBIF abundance	Abundance (res 250m)
Brosimum alicastrum	69	34
Brosimum guianense	27	13
Brosimum lactescens	22	10
Brosimum utile	32	20
Brunellia costaricensis	46	15
Bursera simaruba	193	141
Bursera tomentosa	27	15
Byrsonima arthropoda	12	0
Byrsonima crassifolia	136	82
Calatola costaricensis	93	31
Calliandra trinervia	33	0
Calophyllum brasiliense	62	27
Calycophyllum candidissimum	64	38
Carapa guianensis	29	18
Caryocar costaricense	26	19
Casearia arborea	52	17
Casearia corymbosa	107	36
Casearia sylvestris	92	34
Casearia tacanensis	61	18
Cassia grandis	67	39
Cassipourea elliptica	104	28
Castilla elastica	55	26
Castilla tunu	30	15
Cecropia angustifolia	68	36
Cecropia insignis	62	44
Cecropia obtusifolia	189	151
Cecropia peltata	130	107
Cedrela tonduzii	22	14
Celtis schippii	12	0
Cenostigma eriostachys	20	12
Chimarrhis latifolia	32	14
Chimarrhis parviflora	35	13
Chionanthus panamensis	10	0
Chomelia microloba	20	0
Chomelia spinosa	64	21
Chromolucuma congestifolia	12	0
Chrysochlamys allenii	64	20
Chrysochlamys glauca	142	39
Chrysophyllum brenesii	69	19
Citharexylum costaricense	10	0
Clarisia biflora	57	21
Clarisia racemosa	10	0
Cleidion castaneifolium	39	0
Clethra consimilis	24	0
Clethra costaricensis	74	26

Species	GBIF abundance	Abundance (res 250m)
Clethra lanata	55	20
Cleyera theaeoides	66	18
Coccoloba tuerckheimii	51	16
Cochlospermum vitifolium	144	92
Colubrina spinosa	62	22
Compsoneura excelsa	54	18
Conceveiba pleiostemona	31	10
Cordia alliodora	54	27
Cordia bicolor	30	0
Cordia cymosa	59	25
Cordia megalantha	15	0
Cordia panamensis	39	14
Cornutia pyramidata	99	43
Couma macrocarpa	10	0
Couratari guianensis	21	0
Croton draco	63	36
Croton schiedeanus	100	41
Croton smithianus	14	0
Cupania glabra	38	15
Cupania guatemalensis	45	15
Cupania juglandifolia	15	0
Cynometra retusa	32	11
Damburneya smithii	19	0
Dendropanax arboreus	84	26
Dendropanax caucanus	11	0
Dendropanax globosus	36	11
Dialium guianense	33	14
Diospyros juruensis	16	0
Diphysa americana	27	18
Dipteryx panamensis	29	20
Drimys granadensis	134	62
Drypetes brownii	21	0
Dussia macroprophyllata	29	14
Dystovomita paniculata	25	0
Elaeagia auriculata	39	20
Elaeagia glossostipula	13	0
Elaeoluma glabrescens	13	0
Enterolobium cyclocarpum	108	86
Erythrina poeppigiana	35	29
Escallonia myrtilloides	63	30
Eugenia hiraeifolia	47	14
Ferdinandusa panamensis	40	13
Ficus costaricana	60	25
Ficus crassiuscula	18	12
Ficus crocata	19	0

Species	GBIF abundance	Abundance (res 250m)
Ficus insipida	42	31
Ficus maxima	31	15
Ficus obtusifolia	50	22
Ficus tonduzii	38	19
Garcinia madruno	19	12
Gliricidia sepium	69	49
Goethalsia meiantha	23	17
Graffenrieda galeottii	31	15
Grias cauliflora	27	16
Guarea glabra	192	50
Guarea guidonia	72	11
Guarea kunthiana	48	14
Guarea rhopalocarpa	97	26
Guarea tonduzii	36	0
Guatteria aeruginosa	88	24
Guatteria oliviformis	62	20
Guatteria ucayalina	13	0
Guazuma ulmifolia	109	63
Guettarda macrosperma	37	12
Gymnanthes riparia	41	10
Gyrocarpus jatrophifolius	28	0
Hampea appendiculata	92	34
Handroanthus ochraceus	48	33
Hasseltia floribunda	19	10
Hasseltia guatemalensis	45	0
Hauya elegans	25	0
Hedyosmum bonplandianum	129	40
Hedyosmum goudotianum	47	15
Heisteria concinna	33	17
Heliocarpus americanus	24	0
Heliocarpus appendiculatus	37	12
Hernandia didymantha	12	0
Hieronyma alchorneoides	28	14
Hieronyma oblonga	119	28
Hirtella triandra	83	24
Hura crepitans	86	61
Hymenaea courbaril	55	31
Ilex fortunensis	27	0
Ilex lamprophylla	31	14
Ilex pallida	39	0
Inga barbourii	15	0
Inga laevigata	35	0
Inga leonis	19	0
Inga marginata	74	24
Inga mortoniana	16	0

Species	GBIF abundance	Abundance (res 250m)
Inga oerstediana	49	25
Inga punctata	109	31
Inga sapindoides	65	24
Inga thibaudiana	39	12
Inga venusta	26	10
Inga vera	88	44
Jacaranda copaia	15	12
Jacaratia dolichaula	40	20
Karwinskia calderonii	18	0
Lacistema aggregatum	94	34
Ladenbergia brenesii	36	10
Laplacea fructicosa	14	0
Leptolobium panamense	26	12
Licaria misantlae	23	0
Lippia myriocephala	10	0
Lonchocarpus acuminatus	25	0
Lonchocarpus costaricensis	14	0
Lonchocarpus felipei	32	14
Lonchocarpus ferrugineus	18	0
Lonchocarpus guatemalensis	26	12
Lonchocarpus macrophyllus	23	0
Lonchocarpus minimiflorus	36	14
Lonchocarpus monteviridis	12	0
Lonchocarpus parviflorus	13	0
Lonchocarpus rugosus	45	14
Luehea candida	43	21
Luehea seemannii	47	21
Luehea speciosa	40	13
Lunania mexicana	38	11
Lysiloma auritum	15	0
Lysiloma divaricatum	33	14
Mabea occidentalis	43	18
Maclura tinctoria	55	27
Macrohasseltia macroterantha	31	12
Magnolia poasana	28	10
Manilkara chicle	30	12
Manilkara staminodella	14	0
Maranthes panamensis	11	0
Marila laxiflora	17	0
Matisia pacifica	19	0
Matudaea trinervia	26	0
Meliosma allenii	22	0
Meliosma glabrata	91	21
Meliosma idiopoda	92	21
Meliosma vernicosa	16	0

Species	GBIF abundance	Abundance (res 250m)
Mespilodaphne veraguensis	79	29
Metteniusa tessmanniana	31	0
Miconia affinis	146	46
Miconia bigibbosa	14	0
Miconia biperulifera	33	12
Miconia brenesii	74	15
Miconia brevitheca	17	0
Miconia conomicrantha	102	33
Miconia conorufescens	70	26
Miconia donaeana	60	17
Miconia durandii	76	17
Miconia elata	45	13
Miconia lasiopoda	52	20
Miconia multispicata	16	0
Miconia prasina	95	22
Miconia schnellii	37	10
Miconia tonduzii	165	52
Minquartia guianensis	29	27
Morisonia pittieri	18	0
Mortoniodendron anisophyllum	92	18
Myrcia chytraculia	13	0
Myrcia splendens	174	40
Myrcianthes fragrans	48	13
Myriocarpa longipes	106	50
Myrospermum frutescens	18	0
Myrsine coriacea	139	45
Nectandra membranacea	44	15
Nectandra reticulata	19	0
Ocotea atirrensis	109	34
Ocotea austinii	18	0
Ocotea insularis	82	31
Ocotea laetevirens	42	17
Ocotea macrophylla	39	10
Ocotea stenoneura	17	0
Oreomunnea mexicana	19	0
Oreomunnea pterocarpa	26	14
Oreopanax xalapensis	60	23
Otoba novogranatensis	43	21
Pachira aquatica	114	63
Panopsis costaricensis	45	16
Peltogyne purpurea	15	0
Pentaclethra macroloba	110	68
Pentagonia costaricensis	27	0
Pera arborea	20	0
Perebea hispidula	47	13

Species	GBIF abundance	Abundance (res 250m)
Perrottetia longistylis	38	11
Persea americana	102	82
Persea caerulea	11	0
Persea schiedeana	24	16
Phyllanthus skutchii	18	0
Piptocoma discolor	18	0
Piscidia carthagenensis	14	0
Platymiscium curuense	20	0
Pleuranthodendron lindenii	24	11
Pleurothyrium palmanum	11	0
Pochota fendleri	125	87
Podocarpus oleifolius	49	15
Posoqueria latifolia	138	67
Poulsenia armata	19	10
Pourouma bicolor	45	26
Pourouma minor	31	15
Pouteria laevigata	12	0
Pouteria torta	32	15
Protium confusum	42	17
Protium panamense	12	0
Protium pittieri	27	15
Protium ravenii	42	19
Prumnopitys standleyi	40	22
Pseudolmedia glabrata	29	14
Pseudosamanea guachapele	24	10
Psychotria berteroana	111	41
Pterocarpus michelianus	30	0
Pterocarpus officinalis	22	14
Pterocarpus rohrii	22	12
Quercus corrugata	21	0
Quercus costaricensis	65	34
Quercus insignis	63	38
Quercus oleoides	50	27
Quercus sapotifolia	89	27
Quetzalia occidentalis	35	0
Rehdera trinervis	78	23
Rinorea dasyadena	35	12
Ruagea glabra	52	13
Ruptiliocarpon caracolito	41	16
Sacoglottis trichogyna	16	0
Samanea saman	70	45
Sapium glandulosum	53	20
Saurauia montana	184	59
Schizolobium parahyba	23	20
Sciodaphyllum pittieri	44	18

Species	GBIF abundance	Abundance (res 250m)
Sebastiania pavoniana	27	0
Senna papillosa	87	29
Sideroxylon capiri	59	26
Sideroxylon portoricense	10	0
Simarouba amara	31	22
Simarouba glauca	29	0
Simira maxonii	24	11
Sloanea medusula	20	0
Sloanea terniflora	72	23
Sloanea zuliaensis	27	0
Solenandra mexicana	18	0
Sorocea affinis	33	13
Sorocea pubivena	64	21
Sorocea trophoides	68	23
Spondias mombin	60	31
Spondias purpurea	52	35
Staphylea occidentalis	164	47
Stephanopodium costaricense	15	0
Sterculia apetala	46	26
Stryphnodendron microstachyum	31	14
Styrax argenteus	43	16
Swartzia simplex	46	25
Swietenia macrophylla	31	17
Symphonia globulifera	140	68
Symplocos serrulata	26	0
Tabebuia rosea	84	60
Tabernaemontana donnell-smithii	124	57
Tabernaemontana glabra	61	28
Tabernaemontana longipes	143	38
Tachigali costaricensis	28	0
Talisia nervosa	14	0
Tapirira guianensis	17	0
Tapirira mexicana	28	13
Terminalia oblonga	48	28
Tetrathylacium johansenii	13	0
Tetrathylacium macrophyllum	29	15
Tetrorchidium euryphyllum	71	17
Thouinidium decandrum	32	13
Ticodendron incognitum	74	37
Trichilia americana	48	18
Trichilia martiana	82	29
Trichilia pleeana	13	0
Trichilia septentrionalis	13	0
Trichospermum galeottii	60	16

Species	GBIF abundance	Abundance (res 250m)
Triplaris melaenodendron	57	22
Trophis racemosa	95	30
Unonopsis pittieri	17	0
Verbesina oerstediana	36	0
Viburnum costaricanum	126	47
Virola koschnyi	39	19
Virola montana	11	0
Virola nobilis	33	0
Virola sebifera	57	23
Vismia baccifera	131	57
Vismia macrophylla	49	24
Vitex cooperi	48	26
Vochysia allenii	11	0
Vochysia ferruginea	62	30
Vochysia guatemalensis	42	24
Warszewiczia coccinea	123	71
Weinmannia pinnata	77	18
Xylopia sericea	44	13
Xylopia sericophylla	14	0
Zanthoxylum acuminatum	56	16
Zanthoxylum setulosum	47	17
Zinowiewia integerrima	77	21

Table S2. Presentation of the fifteen class-level landscape metrics calculated for developing an anthropogenic pressure index for each class of interest.

Metric	Name	Unit	Definition
minDist	Minimal distance	m	Measures the distance to the nearest patch of the class.
area_CV	Patch area (coefficient of variation)	%	Measures the area of the class's patches.
area_mean	Patch area (mean)	m²	
ca	Total class area	m²	Corresponds to the total area occupied by all class's patches in the landscape.
clumpy	Clumpiness index	_	Measures the degree of spatial aggregation of a patch class relative to a random distribution.
cohesion	Patch cohesion index	%	Measures the degree of physical connectivity of a patch class within the landscape.
ed	Edge density	m/ha	Corresponds to the sum of the lengths of all edge segments involving patches of the class, divided by the total landscape area.
frac_cv	Fractal dimension index (cv)	%	Corresponds to the shape-complexity index of the class's patches.
frac_mean	Fractal dimension index (mean)	_	
lsi	Landscape shape index	_	Standardised measure of the total edge length of patch class in the landscape, adjusted by the total landscape area.
mesh	Effective mesh size	m²	Measures the effective mean patch size of a class, weighted by patch area and relative to the total landscape area.
np	Number of patches	_	Corresponds to the number of patches of the given class in the landscape, reflecting the degree of subdivision or fragmentation of that class.
pland	% of Landscape	%	Percentage of the total landscape area occupied by class's patches.
shape_cv	Shape index (cv)	%	Measures the shape complexity of the patches within the class.
shape_mean	Shape index (mean)	_	

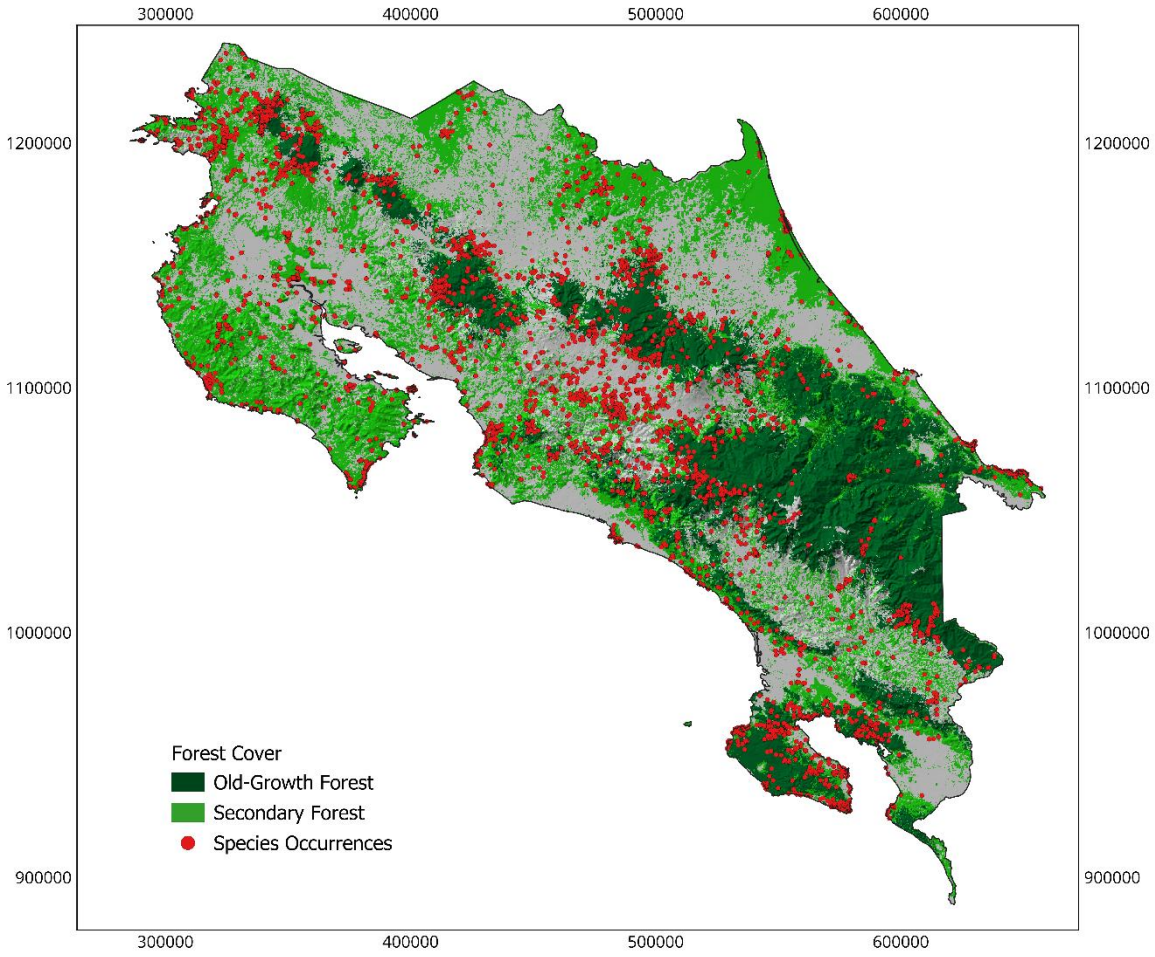

Figure S1. Distribution of occurrences of the 367 species studied from GBIF across Costa Rica's forest cover.

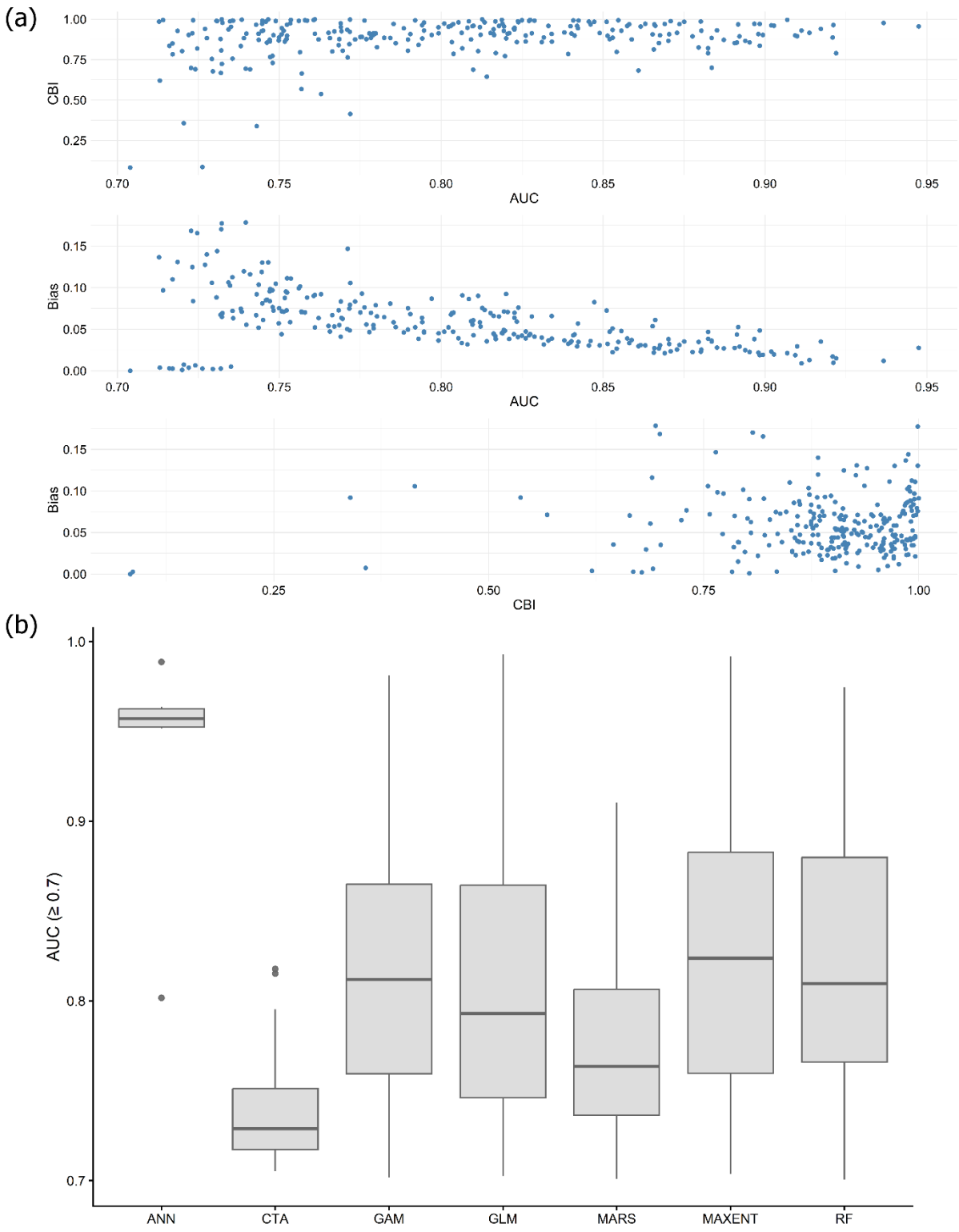

Figure S2. Performance evaluation of ESDMs: (a) Relationships between the performance evaluation metrics of the SDMs for the 254 modelled species: AUC, CBI, and bias. (b) Histogram of the seven modelling algorithms across all species based on AUC values for their inclusion in ensemble models (AUC ≥ 0.7): Generalised Additive Model (GAM), Generalised Linear Model (GLM), Multivariate Adaptive Regression Splines (MARS), Artificial Neural Networks (ANN), Classification Tree Analysis (CTA), Random Forest (RF), and Maximum Entropy (MAXENT). The ANN and CTA algorithms are the

least frequently retained in the final ensemble: ANN is retained for only one species and CTA for 32 species, whereas the other algorithms are retained for between 213 and 247 species.

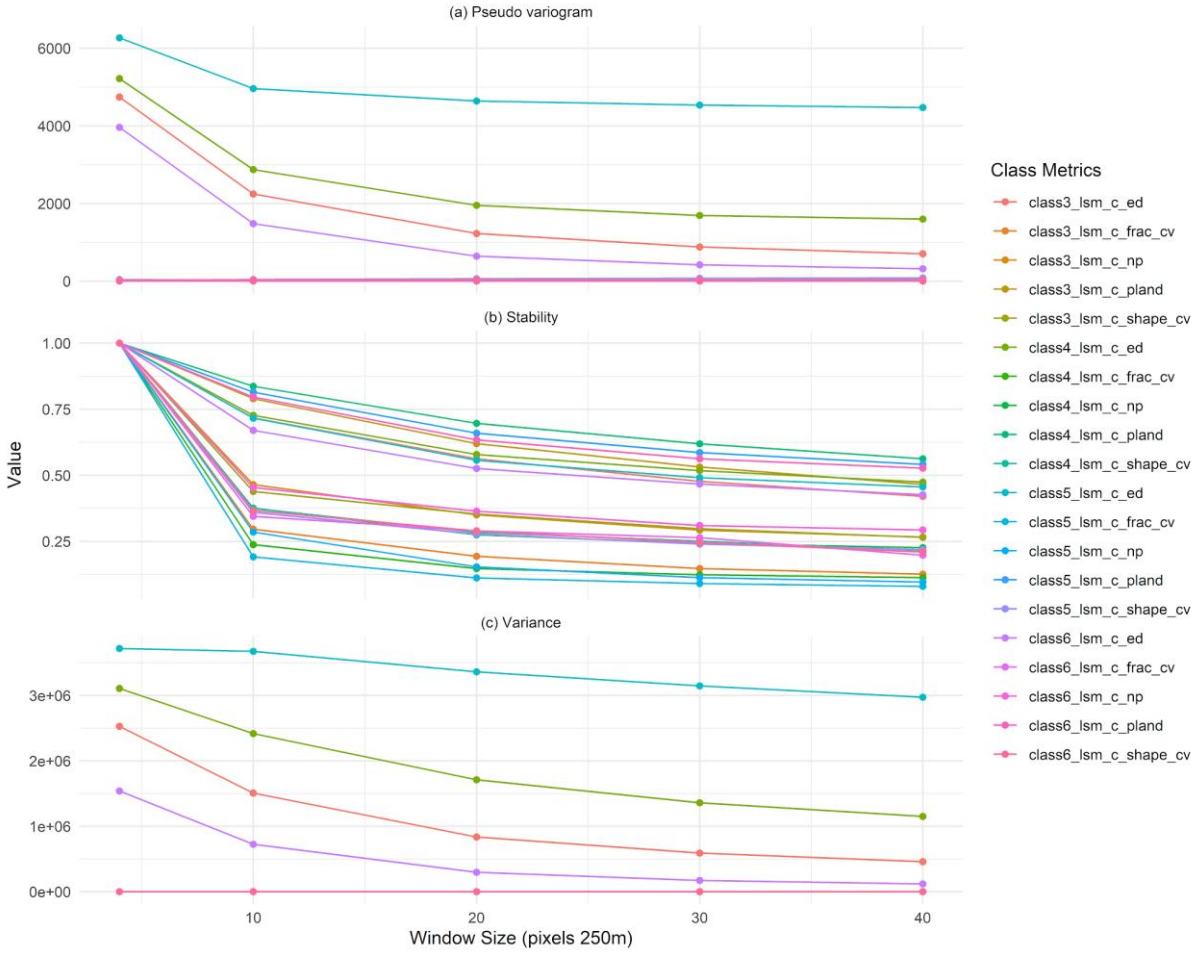

Figure S3. Selection of the optimal focal window size for calculating the spatial structure metrics of anthropogenic LULC classes (class 3 – Forest plantation, class 4 – Crop, class 5 – Pasture, class 6 – Urban area) was performed using three sensitivity tests according to window size (in pixels at a 250 m resolution): (a) Pseudo-variogram illustrating the mean spatial roughness of the metrics; (b) Inter-scale stability of the metrics assessed through correlation with the smallest window (4 pixels – 1 km); (c) Spatial variance of the metrics. The cross-scale analysis indicates that the spatial structure of the landscape changes markedly between 1 km (4 pixels) and 5 km (20 pixels).

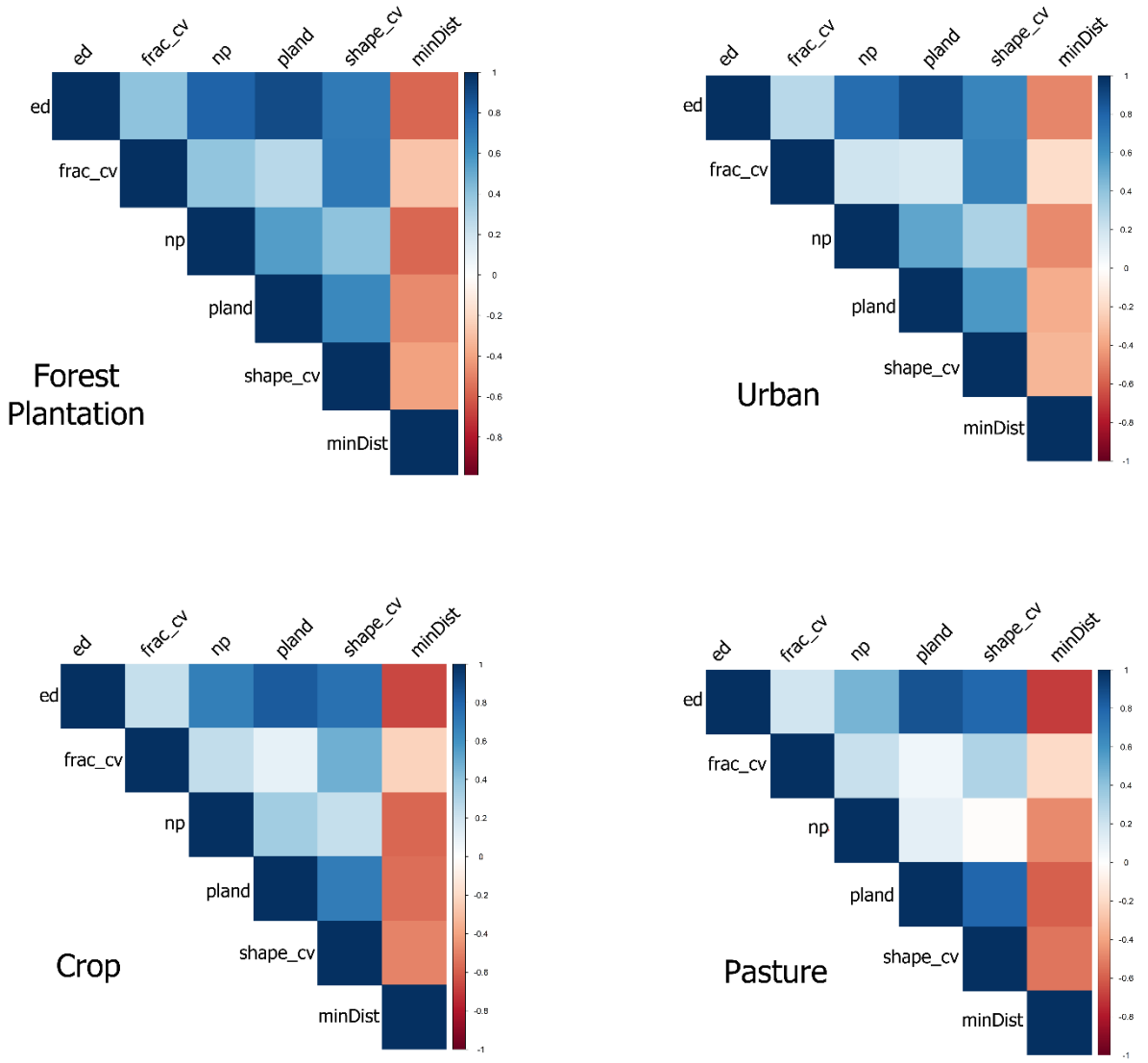

Figure S4. Corrplots showing pairwise correlations (Pearson's r) among class-level landscape metrics computed for four anthropogenic land-use/land-cover classes of interest (urban area, forest plantation, cropland, pasture). These correlation matrices were used to perform a collinearity analysis and to retain a subset of non-collinear and complementary metrics (selection criterion: r<0.8) that are widely recognised as informative in the landscape ecology literature, in order to robustly characterise the relative importance and influence of each anthropogenic class on landscape structure. The same metric-selection procedure was applied to all anthropogenic classes to ensure that the resulting class-specific pressure indices are comparable across classes and can subsequently be combined. Metrics displayed are: edge density (ED), number of patches (NP), percentage of landscape occupied by the class (PLAND), fractal dimension index (coefficient of variation; FRAC_CV), shape index (coefficient of variation; SHAPE_CV), and minimum distance to the class (minDist).

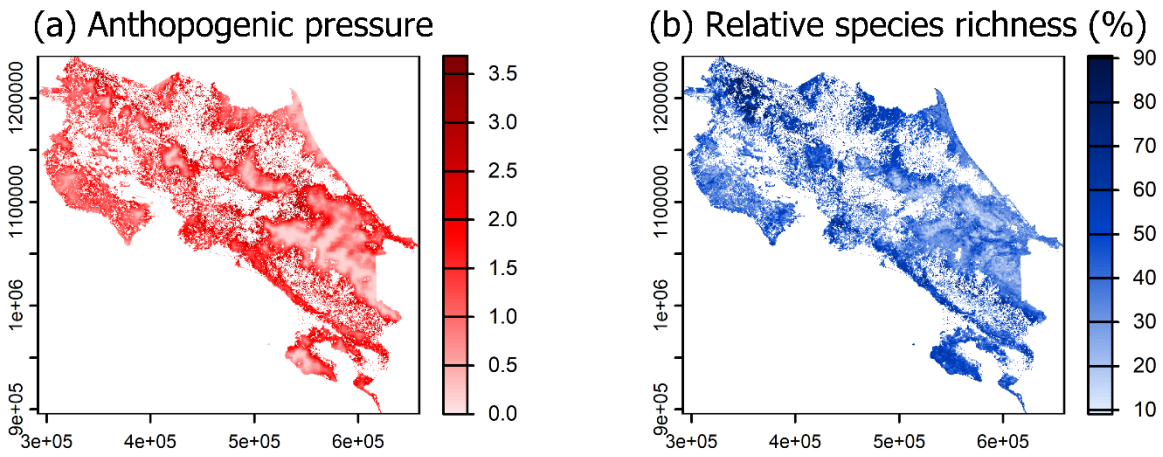

Figure S5. Mapping of (a) aggregated anthropogenic pressure at the landscape scale (within a 5 km radius around each forest pixel), obtained by combining the four pressure indices, and (b) Relative species richness, corresponding to percentage of studied species exhibiting high suitability scores (level 1 and 2 hotspots) within each forest pixel. The local anthropogenic pressure index (a) reveals a strong and continuous accumulation of pressures across a large part of the central and northern regions of the country, as well as in the northern Pacific area. In contrast, the mountainous regions of Talamanca, the forests of the Osa Peninsula, and some isolated Caribbean areas exhibit low to moderate pressure levels. The map of the percentage of species displaying high potential hotspots (b) highlights a clear concentration of hotspots in the mountain ranges, primarily the Guanacaste Range, as well as in the Osa Peninsula and the Fila Costeña Range. These regions show up to 90.55% of species in potential hotspots. Conversely, the Central Valley, the plains along the Pacific and Caribbean coasts, and certain areas of the Central and Talamanca mountain ranges exhibit very low levels of multi-species potential hotspots, with a minimum of 8.66% of species.

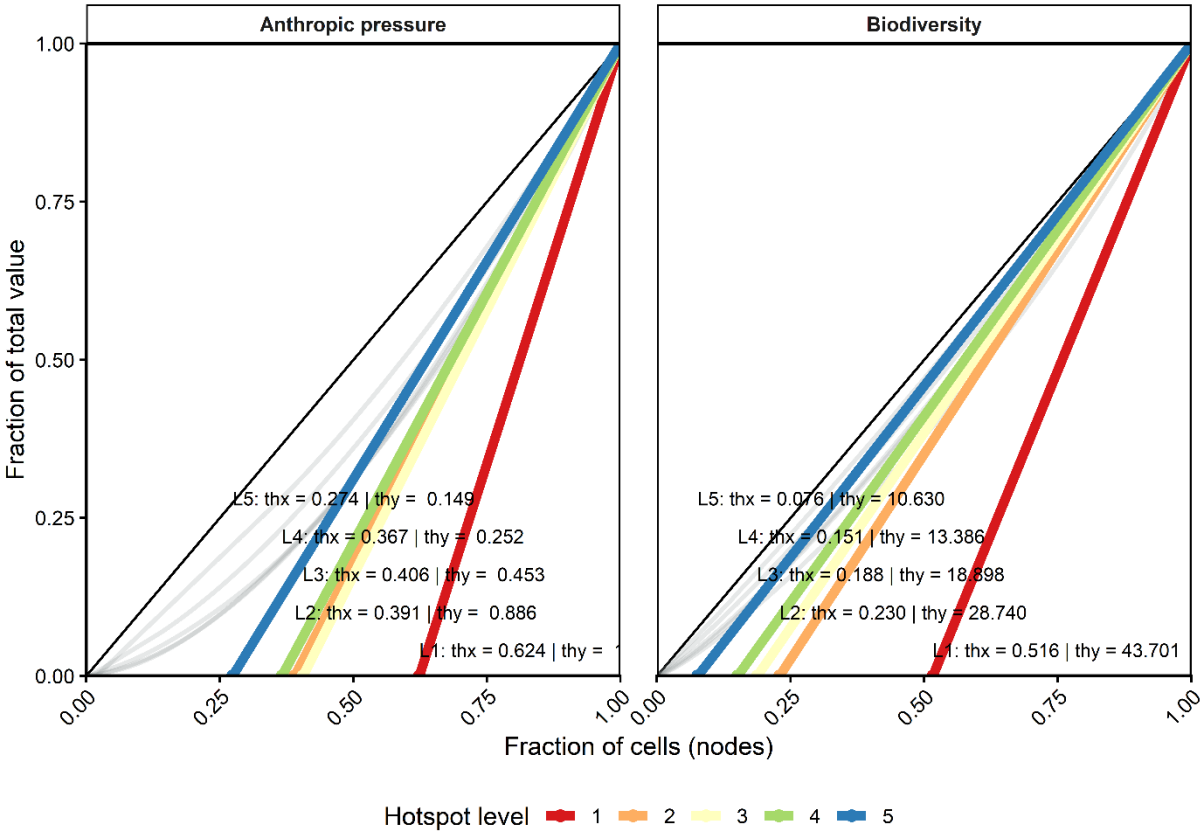

Figure S6. Lorenz curves used for Loubar discretisation of continuous relative species richness and anthropogenic pressure maps into six hotspot levels (level 1 = highest values; level 6 = lowest values).